An Integrated Sensing and Communication System for Time-Sensitive Targets with Random Arrivals

Homa Nikbakht, Yonina C. Eldar, *Fellow, IEEE*, and H. Vincent Poor, *Life Fellow, IEEE*

***Abstract*—In 6G networks, integrated sensing and communication (ISAC) is envisioned as a key technology that enables wireless systems to perform joint sensing and communication using shared hardware, antenna(s) and spectrum. ISAC designs facilitate emerging applications such as digital twins, smart cities and autonomous driving. Such applications also demand ultra-reliable and low-latency communication (URLLC), a feature that was first introduced in 5G and is expected to be further enhanced in 6G. Thus, an ISAC-enabled URLLC system can prioritize critical and time-sensitive targets and ensure information delivery under strict latency and reliability constraints. We propose a bi-static multiple-input multiple-output (MIMO) ISAC system to detect the arrival of URLLC messages and prioritize their delivery. In this system, a dual-function base station (BS) communicates with a user equipment (UE) and a sensing receiver (SR) is deployed to collect echo signals reflected from a target of interest. The BS regularly transmits messages of enhanced mobile broadband (eMBB) services to the UE. During each eMBB transmission, if the SR senses the presence of a target of interest, it immediately triggers the transmission of an additional URLLC message. To reinforce URLLC transmissions, we propose a dirty-paper coding (DPC)-based technique that mitigates the interference of both eMBB and sensing signals. To decode the eMBB message, we consider two approaches for handling the URLLC interference: treating interference as noise (TIN) and successive interference cancellation (SIC). For this system, we formulate the rate-reliability-detection trade-off in the finite blocklength (FBL) regime by evaluating the communication rate of the eMBB transmissions, the reliability of the URLLC transmissions and the probability of the target detection. Our numerical analysis show that our proposed DPC-based ISAC scheme significantly outperforms power-sharing based ISAC and traditional time-sharing schemes. In particular, it achieves higher eMBB transmission rate while satisfying both URLLC and sensing constraints.**

I. Introduction

Integrated sensing and communication (ISAC) is enabled by higher frequency bands, wider bandwidths and denser distributions of massive antenna arrays. Such integration is mutually beneficial to sensing and communication tasks [2]–[4]. On the one hand, the radio wave transmission and reflection can be used to sense the environment and thus the entire communication network can serve as a sensor. On the other hand, the capabilities of high-accuracy localization, imaging, and environment reconstruction obtained from sensing can improve communication performance. ISAC designs thus offer various use cases for autonomous driving, smart factories, and other environment-aware scenarios in 6G communication networks [5]–[9].

Many ISAC use cases also require ultra-reliable and low-latency communication (URLLC), a feature introduced in 5G and is expected to evolve further in 6G [10]–[13]. For example, in autonomous driving, ISAC plays a crucial role in detecting targets, including pedestrians and vehicles and delivering sensing information to users. URLLC is essential for ensuring the timely delivery of critical road safety information [14]. In particular, URLLC ensures 99.99% reliability at a maximum end-to-end delay of no more than one millisecond, which is essential for many 5G and 6G applications, including industrial automation, intelligent transportation, and telemedicine [15]–[19].

Despite progress in achieving the required latency and reliability, 5G URLLC still does not meet all key performance metrics needed for diverse mission-critical applications. One of the main challenges arises from the random generation nature of URLLC services, as their generation is often linked to the occurrence of critical, time-sensitive events in the environment. Consequently, their arrival time becomes unpredictable for transmitting and receiving units. Another challenge is the coexistence of URLLC services with other 5G/6G services such as enhanced mobile broadband (eMBB) that depend largely on high transmission rate and are less sensitive to delay. Different coexistence strategies have been studied in the literature [20]–[24]. For example, [21] proposes a puncturing strategy (also known as time-sharing) in which the on-going eMBB transmission stops upon the arrival of URLLC messages. The work in [22] shows that a superposition coding strategy in which the transmitter simply sends a linear combination of eMBB and URLLC signals while sharing the total transmit power between the two services outperforms the puncturing strategy. A dirty-paper coding (DPC) [25]–[27] based joint transmission strategy is proposed in [23] which also outperforms the puncturing technique. Theses studies either assume a deterministic model or a random model with Bernoulli distribution for the arrival of URLLC messages [23], which have shortcomings in offering a practical model for the stochastic nature of this type of services. Therefore, they do not provide an effective model to address both challenges.

In this work, we address these challenges by proposing a bi-static MIMO ISAC-enabled URLLC system that supports the coexistence of URLLC with eMBB services while using its own sensory data to trigger URLLC transmissions with no assumption on their arrival distribution. In the proposed system, the eMBB message arrives at the beginning of the transmission slot and its transmission lasts over the entire slot. Whereas, transmission of a URLLC message is triggered only when the SR detects the presence of a target.

To enable real-time joint sensing and communication in this

Part of this work is accepted for presentation at the IEEE International Symposium on Information Theory (ISIT), 2025 [1].

system, we divide the eMBB transmission slot into smaller blocks. In each block, the base station (BS) transmits dual-function signals performing simultaneous communication and sensing tasks. If the SR senses the presence of a target, it triggers the transmission of an additional URLLC message over the next immediate block. Each block thus is either with *no URLLC* or *with URLLC* depending on whether a target is detected in the previous block. In blocks with no URLLC, we generate the dual function signal using DPC to precancel the interference of sensing signal from the eMBB transmission. In blocks with URLLC, to increase the reliability of the URLLC transmission, we also propose a DPC based method to generate the dual function signal. In this method, we first precancel the interference of the sensing signal from the eMBB transmission, and then precancel the interference of both eMBB and sensing signals from the URLLC transmission. After each block, the UE attempts to decode a URLLC message using a threshold decoder.

The UE decodes the eMBB message after the entire transmission slot. To handle URLLC interference on the eMBB transmission, we consider two approaches: treating interference as noise (TIN), and successive interference cancellation (SIC). In the TIN approach, the decoding of the eMBB message depends on the detection of URLLC messages sent over all blocks of the transmission slot. Under the SIC approach, prior to the decoding of the eMBB message, the UE first mitigates the interference from correctly decoded URLLC messages across all blocks. Therefore, successful eMBB decoding relies on both the accurate detection and correct decoding of URLLC messages in all blocks. For this system, we optimize the dual-function transmit waveform to maximize the eMBB transmission rate, while ensuring that the URLLC decoding error probability remains below a threshold and the target detection probability exceeds a threshold across all blocks.

We compare our proposed DPC-based scheme with two baseline schemes: time-sharing and power-sharing schemes. Through numerical analyses we show that our proposed DPC-based ISAC scheme outperforms the power-sharing and the time-sharing schemes by achieving higher eMBB rate while accommodating the URLLC constraints and the sensing constraints of the target detection. Our numerical analysis also demonstrate the rate-reliability-detection performance trade-off under both the TIN and SIC approaches. The results show that when there is a high reliability constraint on the URLLC transmissions, the SIC approach outperforms the TIN approach by achieving higher eMBB transmission rate while satisfying the sensing constraints of the target detection. However, the performance gap between the two approaches decreases as the URLLC reliability constraint becomes less stringent. Our proposed ISAC-enabled URLLC system thus effectively addresses both the coexistence and the random nature generation challenges of URLLC services while outperforming the baseline time-sharing and power-sharing based systems.

The rest of this paper is organized as follows. Section II describes the general problem setup. Section III presents our coding schemes and our target detection strategy. Section IV discusses our main results. Section VI concludes the paper. Technical proofs are deferred to appendices.

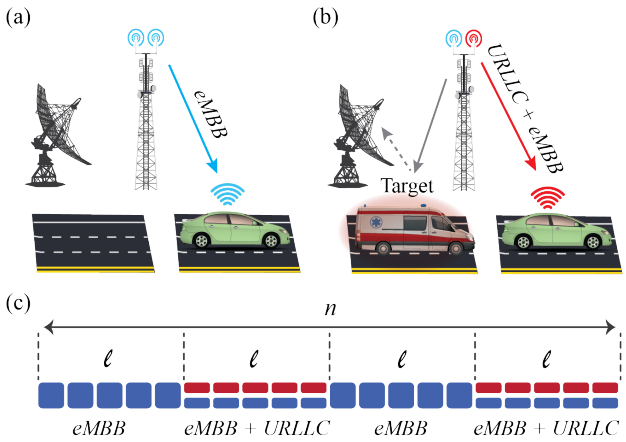

Fig. 1: An illustration of the system model: (a) no target is detected, (b) detection of a target, (c) example of transmission blocks with $\eta = 4$.

II. Problem Setup

We consider a bi-static MIMO ISAC system where a BS is communicating with a UE and simultaneously wishes to sense a target of interest. A SR is deployed to collect echo signals reflected from a target. We assume that the UE is not within the SR sensing range. Hence, the SR does not receive echo signals from the UE. The BS is equipped with t transmit antennas, the UE and the SR each are equipped with r receive antennas. The BS communicates both eMBB and URLLC type messages to the UE. Assume n is the total communication frame length. The BS regularly transmits the eMBB message over the entire n channel uses. We divide n into η blocks each of length ℓ (i.e., $n = \eta \cdot \ell$), as in Fig. 1. The sensing task is performed across all η blocks. In each block b, if the SR senses the presence of a target, it triggers the transmission of an additional URLLC message in the next immediate block. We assume that the SR and the BS can communicate over an interference-free backhaul link. In each block b, the BS thus forms its dual-function transmit signal adaptively based on the target detection outcome in the preceding block $b-1$. In the following sections, we explain the procedures for sensing, adaptive dual-function signal generation, and communication in such blocks.

A. Target Echo Signal Model

The sensing task is performed across all blocks. In a given block $b \in [\eta]$ with $[\eta] := \{1, \ldots, \eta\}$, the SR receives the reflected echo signal $\mathbf{Y}_{b,s} = [\boldsymbol{Y}_{b,s,1} \ldots \boldsymbol{Y}_{b,s,r}] \in \mathbb{C}^{\ell \times r}$. Upon observing $\mathbf{Y}_{b,s}$, the goal of the SR is to detect the presence of a target. The target detection problem in each block thus is formulated by defining the following two hypotheses:

$$\mathcal{H}_0 : \mathbf{Y}_{b,s} = \mathbf{N}_{b,s}, \tag{1}$$

$$\mathcal{H}_1 : \mathbf{Y}_{b,s} = \mathbf{X}_b \mathbf{H}_{b,s} + \mathbf{N}_{b,s}, \tag{2}$$

where $\mathbf{H}_{b,s} \in \mathbb{C}^{t \times r}$ is the target channel response matrix, $\mathbf{N}_{b,s} \in \mathbb{C}^{\ell \times r}$ is additive noise matrix with each entry having

zero mean and unit variance, and $\mathbf{X}_b \in \mathbb{C}^{\ell\times r}$ is the dual-function signal transmitted by the BS. We will explain shortly how this signal is formed. The optimal detector for this problem is the likelihood ratio test (LRT) [28] and is given by

$$T_b = \log\left(\prod_{j=1}^{q}\frac{f\left(\boldsymbol{Y}_{b,s,j}|\mathcal{H}_1\right)}{f\left(\boldsymbol{Y}_{b,s,j}|\mathcal{H}_0\right)}\right)\underset{\mathcal{H}_0}{\overset{\mathcal{H}_1}{\gtrless}}\delta \tag{3}$$

where $f\left(\boldsymbol{Y}_{b,s,j}|\mathcal{H}_0\right)$ and $f\left(\boldsymbol{Y}_{b,s,j}|\mathcal{H}_1\right)$ are the probability density functions (pdf) of the observation vector under the null and alternative hypotheses, respectively, and $q := \min\{r,t\}$. We denote the target detection and false alarm probabilities of block b by $P_{b,\mathsf{D}}$ and $P_{b,\mathrm{FA}}$, respectively, which are

$$P_{b,\mathsf{D}} = \mathbb{P}[T_b > \delta|\mathcal{H}_1], \tag{4a}$$
$$P_{b,\mathrm{FA}} = \mathbb{P}[T_b > \delta|\mathcal{H}_0]. \tag{4b}$$

The threshold δ is set to ensure the desired probability of false alarm. In each block b, we assume that the SR has the full knowledge of the sensing channel state information.

B. Dual-Function Signal Generation

In each block $b \in [\eta]$, the dual-function signal $\mathbf{X}_b$ is generated adaptively depending on whether a target is detected in the preceding block $b-1$. More specifically, the BS transmits the eMBB message m_e across all η blocks, where m_{e} is uniformly drawn from the set $\mathcal{M}_{\mathsf{e}} := \{1,\ldots,M_{\mathsf{e}}\}$. In each block b, the BS transmits an additional URLLC message $m_{b,\mathsf{U}}$ to the UE with probability $P_{b-1,\mathsf{D}}$ which is the target detection probability in block $b-1$. With probability $1-P_{b-1,\mathsf{D}}$ no URLLC message is generated. If present, the message $m_{b,\mathsf{U}}$ is uniformly drawn from the set $\mathcal{M}_{\mathsf{U}} := \{1,\ldots,M_{\mathsf{U}}\}$.

In each block b, the BS thus creates its dual-function signal $\mathbf{X}_b \in \mathbb{C}^{\ell\times t}$ as

$$\mathbf{X}_b = \begin{cases} f_b^{(\ell)}(m_e, m_{b,\mathsf{U}}), & \text{with probability } P_{b-1,\mathsf{D}} \\ f_e^{(\ell)}(m_e), & \text{with probability } 1-P_{b-1,\mathsf{D}}, \end{cases} \tag{5}$$

where $f_e^{(\ell)}$ and $f_b^{(\ell)}$ are encoding functions on appropriate domains. We assume that $P_{0,\mathsf{D}} = 0$, i.e., no URLLC is transmitted over the first block. Denote $\mathbf{X} := [\mathbf{X}_1^T,\ldots,\mathbf{X}_\eta^T]^T$. The input matrix $\mathbf{X}$ is admissible if it belongs to the following set:

$$\mathcal{P}_X(\mathsf{P}) := \left\{\mathbf{X}\in\mathbb{C}^{n\times t} : \mathrm{Tr}\left(\mathbf{X}\mathbf{X}^H\right) \le n\mathsf{P}\right\}, \tag{6}$$

that implies a power constraint on the input matrix $\mathbf{X}$ by upper bounding the trace of $\mathbf{X}\mathbf{X}^H$ with $n\mathsf{P}$. Define

$$\mathcal{B}_{\mathrm{URLLC}} := \{b\in[\eta] : \text{block } b \text{ is with URLLC}\}, \tag{7}$$

as the set of blocks in which an additional URLLC message is generated.

C. Communication Received Signal at the UE

At the end of each block $b\in[\eta]$, the UE receives the signal $\mathbf{Y}_{b,c} = [\boldsymbol{Y}_{b,c,1}\ldots\boldsymbol{Y}_{b,c,r}] \in \mathbb{C}^{\ell\times r}$ from the BS. Assume a MIMO memoryless Gaussian quasi-static fading channel. The channel input-output relation in each block $b\in[\eta]$ is given by

$$\mathbf{Y}_{b,c} = \mathbf{X}_b\mathbf{H}_{b,c} + \mathbf{N}_{b,c}, \tag{8}$$

where $\mathbf{Y}_{b,c} \in \mathbb{C}^{\ell\times r}$ is the communication channel output, $\mathbf{H}_{b,c}\in\mathbb{C}^{t\times r}$ is the communication channel matrix, and $\mathbf{N}_{b,c}\in\mathbb{C}^{\ell\times r}$ is additive noise at the UE whose entries are i.i.d. $\mathcal{N}(0,1)$ and is independent of $\mathbf{H}_{b,c}$. Assume that the channel state information is known at both the BS and the UE. After each block $b\in\mathcal{B}_{\mathrm{URLLC}}$, the UE decodes the transmitted URLLC message $m_{b,\mathsf{U}}$. Thus it produces

$$\hat{m}_{b,\mathsf{U}} = g_{b,u}^{(\ell)}(\mathbf{Y}_{b,c},\mathbf{H}_{b,c}), \tag{9}$$

for some decoding function $g_{b,u}^{(\ell)}$ on appropriate domain. Otherwise, the UE produces $\hat{m}_{b,\mathsf{U}} = 0$ if $b\notin\mathcal{B}_{\mathrm{URLLC}}$. For each message $m_{b,\mathsf{U}}$, the average error probability is defined as

$$\begin{aligned}\epsilon_{b,\mathsf{U}} := {} & P_{b-1,\mathsf{D}}\mathbb{P}[\hat{m}_{b,\mathsf{U}}\neq m_{b,\mathsf{U}}|b\in\mathcal{B}_{\mathrm{URLLC}}] \\ & +(1-P_{b-1,\mathsf{D}})\mathbb{P}[\hat{m}_{b,\mathsf{U}}\neq 0|b\notin\mathcal{B}_{\mathrm{URLLC}}].\end{aligned} \tag{10}$$

After the entire η blocks, the UE decodes its desired eMBB message as:

$$\hat{m}_{\mathsf{e}} = g_{\mathsf{e}}^{(n)}(\mathbf{Y}_{1,c},\ldots,\mathbf{Y}_{\eta,c},\mathbf{H}_{1,c},\ldots,\mathbf{H}_{\eta,c}). \tag{11}$$

where $g_{\mathsf{e}}^{(n)}$ is a decoding function on appropriate domain. The average error probability of the eMBB message m_e is defined as

$$\epsilon_{\mathsf{e}}^{(n)} := \mathbb{P}[\hat{m}_{\mathsf{e}}\neq m_{\mathsf{e}}]. \tag{12}$$

The objective is to optimize the dual-function transmit waveform $\mathbf{X}$ to maximize the eMBB transmission rate, while ensuring that the URLLC decoding error probability $\epsilon_{b,\mathsf{U}}$ remains below a threshold and the target detection probability $P_{b,\mathsf{D}}$ exceeds a threshold across all blocks. In the following Proposition 1, we formulate the corresponding optimization problem as the rate-reliability-detection trade-off.

Proposition 1: Given n,η and P, let $\mathsf{R}_e := \frac{\log M_{\mathsf{e}}}{n}$ be the eMBB transmission rate. The *rate-reliability-detection trade-off* is

$$\max_{f_{\mathbf{X}}(\mathbf{x})\in\mathcal{P}_X(\mathsf{P})} \quad \mathsf{R}_{\mathsf{e}} \tag{13a}$$
$$\text{subject to} \quad \epsilon_{\mathsf{e}}^{(n)} \le \epsilon_{\mathsf{e}}, \tag{13b}$$
$$\epsilon_{b,\mathsf{U}} \le \epsilon_{\mathsf{U}}, \quad \forall b\in[\eta], \tag{13c}$$
$$P_{b,\mathsf{D}} \ge \mathsf{P}_{\mathsf{D}}, \quad \forall b\in[\eta], \tag{13d}$$

where $\mathcal{P}_X(\mathsf{P})$ is defined in (6).

III. Coding Scheme

In this section, we propose a coding scheme to design the dual-function sensing and communication signal $\mathbf{X}$ in different transmission blocks with the objective of Proposition 1. Due to URLLC requirements, we perform our analysis in the finite

blocklength (FBL) regime [29]–[31]. In terms of the choice of input distribution, to improve the FBL analysis of power-constrained channels, our analysis relies on the use of power-shell codebooks. A power-shell codebook of length ℓ consists of codewords that are uniformly distributed on the centered $(\ell-1)$-dimensional sphere with radius $\sqrt{\ell \mathsf{P}}$ where P is the power constraint. According to Shannon's observation, the optimal decay of the probability of error near capacity of the point-to-point Gaussian channel is achieved by codewords on the power-shell [32].

Codewords are generated such that the total transmit power satisfies the power constraint (6) over the η blocks. Therefore, in each block $b \notin \mathcal{B}_{\text{URLLC}}$, we choose a power sharing parameter $\beta_{s,1} \in [0,1]$ to allocate $(1-\beta_{s,1})\mathsf{P}$ to the sensing task and the remaining $\beta_{s,1}\mathsf{P}$ to the communication task of transmitting only the eMBB message. In each block $b \in \mathcal{B}_{\text{URLLC}}$, we choose power sharing parameters $\beta_u, \beta_{s,2} \in [0,1]$. We allocate $\beta_u \mathsf{P}$ to the URLLC transmission, $\beta_{s,2}(1-\beta_u)\mathsf{P}$ to the eMBB transmission and the remaining $(1-\beta_{s,2})(1-\beta_u)\mathsf{P}$ to the sensing task.

Denote a centered ℓ-dimensional sphere of radius r by $\mathsf{S}_\ell(r)$. For each block $b \in [\eta]$ and for each transmit antenna $j \in [t]$, we generate the following codewords that are uniformly distributed on the power-shell.

- For each $v \in [M_v]$ and each realization $m \in [M_{\mathsf{U}}]$, generate codewords $\boldsymbol{V}_{b,j}(m,v)$ by picking them uniformly over $\mathsf{S}_\ell\left(\sqrt{\ell(\beta_u + \alpha_u^2(1-\beta_u))\mathsf{P}}\right)$ with $\alpha_u \in [0,1]$.
- For each $s \in [M_{\mathsf{s}}]$ and each realization $m' \in [M_{\mathsf{e}}]$, randomly draw two codewords: a codeword $\boldsymbol{S}_{b,j}^{(1)}(m',s)$ uniformly distributed on $\mathsf{S}_\ell\left(\sqrt{\ell(\beta_{s,1} + \alpha_{s,1}^2(1-\beta_{s,1}))\mathsf{P}}\right)$ with $\alpha_{s,1} \in [0,1]$; and a codeword $\boldsymbol{S}_{b,j}^{(2)}(m',s)$ uniformly distributed on $\mathsf{S}_\ell\left(\sqrt{\ell(1-\beta_u)(\beta_{s,2} + \alpha_{s,2}^2(1-\beta_{s,2}))\mathsf{P}}\right)$, with $\alpha_{s,2} \in [0,1]$.
- For each $s \in [M_{\mathsf{s}}]$, randomly draw two codewords: a codeword $\boldsymbol{X}_{b,j}^{(\mathsf{s},1)}(s)$ uniformly distributed on $\mathsf{S}_\ell\left(\sqrt{\ell(1-\beta_{s,1})\mathsf{P}}\right)$; and a codeword $\boldsymbol{X}_{b,j}^{(\mathsf{s},2)}(s)$ uniformly distributed on $\mathsf{S}_\ell\left(\sqrt{\ell(1-\beta_u)(1-\beta_{s,2})\mathsf{P}}\right)$.

All codewords are chosen independently of each other. We assume that in each block b, the SR has a full knowledge about the auxiliary codewords $\boldsymbol{X}_{b,j}^{(\mathsf{s},1)}$ and $\boldsymbol{X}_{b,j}^{(\mathsf{s},2)}$ for all $j \in [q]$. We thus denote this codewords as sensing signals. However, the SR has no knowledge about the URLLC codeword $\boldsymbol{V}_{b,j}$ and the eMBB codewords $\boldsymbol{S}_{b,j}^{(1)}$ and $\boldsymbol{S}_{b,j}^{(2)}$. We denote these codewords as communication signals. In each block $b \in [\eta]$ and for each transmit antenna $j \in [q]$, the dual-function signal $\boldsymbol{X}_{b,j}$ is created by superposing the sensing and communication signals using the DPC technique. Specifically, in each block $b \notin \mathcal{B}_{\text{URLLC}}$, we employ a DPC technique with parameter $\alpha_{s,1} \in [0,1]$ to precancel the interference of the sensing signal from the eMBB transmission. In each block $b \in \mathcal{B}_{\text{URLLC}}$ where the BS has both eMBB and URLLC messages to send, we first precancel the interference of the sensing signal from the eMBB transmission using a DPC with parameter $\alpha_{s,2} \in [0,1]$, and then precancel the interference of both eMBB and sensing signals from the URLLC transmission using a DPC with parameter $\alpha_u \in [0,1]$. In the following sections, we explain encoding, decoding and target detection processes in details.

A. Encoding

1) Encoding at each block $b \notin \mathcal{B}_{URLLC}$: In each block $b \notin \mathcal{B}_{\text{URLLC}}$, for each $j \in [t]$, the BS first picks its sensing signal $\boldsymbol{X}_{b,j}^{(s,1)}(s)$ and then uses DPC to encode its eMBB message m_{e} while precanceling the interference of its own sensing signal. Specifically, it chooses an index s such that the

$$\boldsymbol{X}_{b,j}^{(\mathsf{e},1)} := \boldsymbol{S}_{b,j}^{(1)}(m_{\mathsf{e}}, s) - \alpha_{s,1}\boldsymbol{X}_{b,j}^{(\mathsf{s},1)} \tag{14}$$

lies in the set $\mathcal{D}(\ell\beta_{s,1}\mathsf{P}, \zeta_{s,1})$ for a given $\zeta_{\mathsf{s},1} > 0$ where

$$\mathcal{D}(a,\zeta) := \left\{\boldsymbol{x} : a - \zeta \le \|\boldsymbol{x}\|^2 \le a\right\}. \tag{15}$$

For simplicity, we assume that at least one such a codeword exists. If multiple such codewords exist, the index s is chosen at random from this set, and the BS sends $\mathbf{X}_b = [\boldsymbol{X}_{b,1}, \ldots, \boldsymbol{X}_{b,t}]$ with

$$\boldsymbol{X}_{b,j} = \boldsymbol{X}_{b,j}^{(\mathsf{e},1)} + \boldsymbol{X}_{b,j}^{(\mathsf{s},1)}, \quad j \in [t]. \tag{16}$$

2) Encoding at each block $b \in \mathcal{B}_{URLLC}$: In each block $b \in \mathcal{B}_{\text{URLLC}}$, the BS has both eMBB and URLLC messages to send. For each $j \in [t]$, it first picks its sensing signal $\boldsymbol{X}_{b,j}^{(\mathsf{s},2)}(s)$. It then uses DPC to encode its eMBB message m_{e} while precanceling the interference of its own sensing signal. More specifically it chooses an index s such that

$$\boldsymbol{X}_{b,j}^{(\mathsf{e},2)} := \boldsymbol{S}_{b,j}^{(2)}(m_{\mathsf{e}}, s) - \alpha_{s,2}\boldsymbol{X}_{b,j}^{(\mathsf{s},2)} \tag{17}$$

lies in the set $\mathcal{D}\left(\ell\beta_{s,2}(1-\beta_u)\mathsf{P}, \zeta_{\mathsf{s},2}\right)$ for a given $\zeta_{\mathsf{s},2} > 0$. Then it employs DPC to encode $m_{b,\mathsf{U}}$ while precanceling the interference of its own sensing and eMBB signals $\boldsymbol{X}_{b,j}^{(\mathsf{e},2)} + \boldsymbol{X}_{b,j}^{(\mathsf{s},2)}$. Specifically, it chooses an index v such that the sequence

$$\boldsymbol{X}_{b,j}^{(\mathsf{U})} := \boldsymbol{V}_{b,j}(m_{b,\mathsf{U}}, v) - \alpha_u\left(\boldsymbol{X}_{b,j}^{(\mathsf{e},2)} + \boldsymbol{X}_{b,j}^{(\mathsf{s},2)}\right) \tag{18}$$

lies in the set $\mathcal{D}\left(\ell\beta_u\mathsf{P}, \zeta_u\right)$ for a given $\zeta_u > 0$. If multiple such codewords exist, indices s and v are chosen at random from these sets, and the BS sends $\mathbf{X}_b = [\boldsymbol{X}_{b,1}, \ldots, \boldsymbol{X}_{b,t}]$ with

$$\boldsymbol{X}_{b,j} = \boldsymbol{X}_{b,j}^{(\mathsf{U})} + \boldsymbol{X}_{b,j}^{(\mathsf{e},2)} + \boldsymbol{X}_{b,j}^{(\mathsf{s},2)}, \quad j \in [t]. \tag{19}$$

B. Decoding

1) Decoding of URLLC Messages: At the end of each block $b \in [\eta]$, the UE observes the channel outputs $\mathbf{Y}_{b,c}$:

$$\mathbf{Y}_{b,c} = \begin{cases} (\mathbf{X}_b^{(\mathsf{e},1)} + \mathbf{X}_b^{(\mathsf{s},1)})\mathbf{H}_{b,c} + \mathbf{N}_{b,c} & \text{if } b \notin \mathcal{B}_{\text{URLLC}} \\ (\mathbf{X}_b^{(\mathsf{U})} + \mathbf{X}_b^{(\mathsf{e},2)} + \mathbf{X}_b^{(\mathsf{s},2)})\mathbf{H}_{b,c} + \mathbf{N}_{b,c} & \text{o.w.} \end{cases} \tag{20}$$

Define the information density metric between $\mathbf{y}_{b,c}$ and $\mathbf{v}_b := [\boldsymbol{v}_{b,1}, \ldots, \boldsymbol{v}_{b,q}]$ by:

$$i_b^{(\mathsf{U})}(\mathbf{v}_b; \mathbf{y}_{b,c}) := \log \frac{f_{\mathbf{Y}_{b,c}|\mathbf{V}_b}(\mathbf{y}_{b,c}|\mathbf{v}_b)}{f_{\mathbf{Y}_{b,c}}(\mathbf{y}_{b,c})}. \tag{21}$$

The UE then chooses the pair

$$(m^*, v^*) = \arg\max_{m,v} i_b^{(\mathsf{U})}(\mathbf{v}_b; \mathbf{y}_{b,c}). \tag{22}$$

Given a threshold δ_{U}, if for this pair

$$i_b^{(\mathsf{U})}(\mathbf{v}_b; \mathbf{y}_{b,c}) > \delta_{\mathsf{U}} \tag{23}$$

the UE chooses $(\hat{m}_{b,\mathsf{U}}, \hat{v}) = (m^*, v^*)$. Otherwise the UE declares that no URLLC message has been received and indicates it by setting $\hat{m}_{b,\mathsf{U}} = 0$. Define

$$\mathcal{B}_{\text{detect}} := \{b \in [\eta] : \hat{m}_{b,\mathsf{U}} \neq 0\}, \tag{24}$$

$$\mathcal{B}_{\text{decode}} := \{b \in \mathcal{B}_{\text{detect}} : \hat{m}_{b,\mathsf{U}} = m_{b,\mathsf{U}}\}, \tag{25}$$

where $\mathcal{B}_{\text{detect}}$ denotes the set of blocks in which a URLLC message is detected and $\mathcal{B}_{\text{decode}}$ denotes the set of blocks in which a URLLC message is decoded correctly.

2) Decoding the eMBB Message under the TIN Approach: The UE decodes its eMBB message based on the output of the entire η blocks. Let $\mathbf{Y}_c := [\mathbf{Y}_{1,c}, \ldots, \mathbf{Y}_{\eta,c}]$. Given that the URLLC messages interfere on the eMBB transmissions, under this approach, the UE treats URLLC transmissions as noise. Therefore, the decoding of the eMBB message depends on the detection of URLLC messages sent over the η blocks. Let B_{dt} be the realization of the set $\mathcal{B}_{\text{detect}}$ defined in (24). Also, let $\mathbf{s}_{\mathsf{e},1} := \{\mathbf{s}_b^{(1)}\}_{b \notin B_{\text{dt}}}$, and $\mathbf{s}_{\mathsf{e},2} := \{\mathbf{s}_b^{(2)}\}_{b \in B_{\text{dt}}}$. Given B_{dt}, the UE decodes its eMBB message based on the outputs of the entire n channel uses by looking for an index pair (m', s') such that its corresponding codewords $\{\mathbf{s}_{\mathsf{e},2}(m', s'), \mathbf{s}_{\mathsf{e},1}(m', s')\}$ maximize

$$i_{\text{TIN}}^{(\mathsf{e})}(\mathbf{s}_{\mathsf{e},2}, \mathbf{s}_{\mathsf{e},1}; \mathbf{y}_c | \mathcal{B}_{\text{detect}} = B_{\text{dt}}) :=$$
$$\log \prod_{b \notin B_{\text{dt}}} \frac{f_{\mathbf{Y}_{b,c}|\mathbf{S}_b^{(1)}}(\mathbf{y}_{b,c}|\mathbf{s}_b^{(1)})}{f_{\mathbf{Y}_{b,c}}(\mathbf{y}_{b,c})} + \log \prod_{b \in B_{\text{dt}}} \frac{f_{\mathbf{Y}_{b,c}|\mathbf{S}_b^{(2)}}(\mathbf{y}_{b,c}|\mathbf{s}_b^{(2)})}{f_{\mathbf{Y}_{b,c}}(\mathbf{y}_{b,c})} \tag{26}$$

among all codewords $\{\mathbf{s}_{\mathsf{e},2}(m', s'), \mathbf{s}_{\mathsf{e},1}(m', s')\}$.

3) Decoding the eMBB Message under the SIC Approach: Under this approach, before decoding the eMBB message, the UE first mitigates the interference of correctly decoded URLLC messages over the η blocks. Therefore, the decoding of the eMBB message depends on both the detection of URLLC messages sent over the η blocks and the decoding of such messages. Let B_{dc} be the realization of the set $\mathcal{B}_{\text{decode}}$ defined in (24). Also, let $\mathbf{s}_{\mathsf{e},1} := \{\mathbf{s}_b^{(1)}\}_{b \notin B_{\text{dt}}}$, and $\mathbf{s}_{\mathsf{e},2} := \{\mathbf{s}_b^{(2)}\}_{b \in B_{\text{dt}}}$. Given B_{dt} and B_{dc}, the UE decodes its eMBB message based on the outputs of the entire n channel uses by looking for an index pair (m', s') such that its corresponding codewords $\{\mathbf{s}_{\mathsf{e},2}(m', s'), \mathbf{s}_{\mathsf{e},1}(m', s')\}$ maximize

$$i_{\text{SIC}}^{(\mathsf{e})}(\mathbf{s}_{\mathsf{e},2}, \mathbf{s}_{\mathsf{e},1}; \mathbf{y}_c | \mathcal{B}_{\text{detect}} = B_{\text{dt}}, \mathcal{B}_{\text{decode}} = B_{\text{dc}}) :=$$
$$\log \prod_{b \notin B_{\text{dt}}} \frac{f_{\mathbf{Y}_{b,c}|\mathbf{S}_b^{(1)}}(\mathbf{y}_{b,c}|\mathbf{s}_b^{(1)})}{f_{\mathbf{Y}_{b,c}}(\mathbf{y}_{b,c})} + \log \prod_{b \in B_{\text{dt}} \setminus B_{\text{dc}}} \frac{f_{\mathbf{Y}_{b,c}|\mathbf{S}_b^{(2)}}(\mathbf{y}_{b,c}|\mathbf{s}_b^{(2)})}{f_{\mathbf{Y}_{b,c}}(\mathbf{y}_{b,c})}$$
$$+ \log \prod_{b \in B_{\text{dc}}} \frac{f_{\mathbf{Y}_{b,c}|\mathbf{S}_b^{(2)},\mathbf{V}_b}(\mathbf{y}_{b,c}|\mathbf{s}_b^{(2)}, \mathbf{v}_b)}{f_{\mathbf{Y}_{b,c}|\mathbf{V}_b}(\mathbf{y}_{b,c}|\mathbf{v}_b)} \tag{27}$$

among all codewords $\{\mathbf{s}_{\mathsf{e},2}(m', s'), \mathbf{s}_{\mathsf{e},1}(m', s')\}$.

C. Target Detection

Following the proposed encoding and decoding schemes, the received signal at the SR in the alternative hypothesis in (2) can be reformulated as

$$\mathbf{Y}_{b,s} = \begin{cases} (\mathbf{X}_b^{(\mathsf{e},1)} + \mathbf{X}_b^{(\mathsf{s},1)})\mathbf{H}_{b,s} + \mathbf{N}_{b,s}, & b \notin \mathcal{B}_{\text{URLLC}} \\ (\mathbf{X}_b^{(\mathsf{U})} + \mathbf{X}_b^{(\mathsf{e},2)} + \mathbf{X}_b^{(\mathsf{s},2)})\mathbf{H}_{b,s} + \mathbf{N}_{b,s}, & \text{o.w.} \end{cases} \tag{28}$$

In each block, the SR has the knowledge of the sensing signal but treats the interference of the communication signal as noise.

IV. Main Results

Our main results are presented in Theorem 1 and Theorem 2 where we formulate the optimization problem of Proposition 1 under the TIN and SIC approaches, respectively. Based on our proposed coding scheme in Section III, the design of the dual-function transmit waveform $\mathbf{X}$ reduces to selecting the coding parameters $\boldsymbol{\alpha} := \{\alpha_u, \alpha_{s,1}, \alpha_{s,2}\}$ and $\boldsymbol{\beta} := \{\beta_{\mathsf{U}}, \beta_{s,1}, \beta_{s,2}\}$. Hence, the objective is to maximize the eMBB transmission rate over different value of $\boldsymbol{\beta}$ and $\boldsymbol{\alpha}$ while ensuring that the URLLC decoding error probability $\epsilon_{b,\mathsf{U}}$ remains below a threshold and the target detection probability $P_{b,\mathsf{D}}$ exceeds a threshold across all blocks. To this end, in this section, we first evaluate the URLLC decoding error probability in Lemma 1, the eMBB transmission rate under the TIN and SIC approaches in Lemma 2 and Lemma 3, and the target detection probability in Lemma 4. By combining these lemmas with Proposition 1, we then prove Theorem 1 and Theorem 2.

A. URLLC Decoding Error Probability Analysis

When channel state is known at both the BS and the UE, then by performing a singular value decomposition, the MIMO channel in (8) is transferred into the following set of $q := \min\{t, r\}$ parallel channels

$$\boldsymbol{Y}_{b,c,j} = \boldsymbol{X}_{b,j}\sqrt{\lambda_{b,j}} + \boldsymbol{N}_{b,c,j}, \tag{29}$$

for each $j \in [q]$ and each $b \in [\eta]$. Here, $\lambda_{b,1} \geq \lambda_{b,2} \geq \cdots \geq \lambda_{b,q}$ are the largest q eigenvalues of $\mathbf{H}_{b,c}\mathbf{H}_{b,c}^H$ and $\boldsymbol{N}_{b,c,j} \sim \mathcal{N}(\mathbf{0}, \mathbf{I}_{\ell \times \ell})$ are independent noise vectors. Let $\boldsymbol{\lambda}_b := [\lambda_{b,1}, \ldots, \lambda_{b,q}]$. Also, let $\mathbf{X}_b := [\boldsymbol{X}_{b,1}, \ldots, \boldsymbol{X}_{b,q}]$. In each block $b \in \mathcal{B}_{\text{URLLC}}$, we have the following URLLC decoding error events:

$$\mathcal{E}_{\mathsf{U},1} := \{b \notin \mathcal{B}_{\text{detect}} | b \in \mathcal{B}_{\text{URLLC}}\}, \tag{30}$$

$$\mathcal{E}_{\mathsf{U},2} := \{b \notin \mathcal{B}_{\text{decode}} | b \in \mathcal{B}_{\text{detect}}, b \in \mathcal{B}_{\text{arrival}}\}, \tag{31}$$

which indicate a missed-detection event. Specifically, $\mathcal{E}_{\mathsf{U},1}$ happens when the transmitted URLLC message is not detected and $\mathcal{E}_{\mathsf{U},2}$ happens when the decoded URLLC message does not match the transmitted one. In each block $b \notin \mathcal{B}_{\text{URLLC}}$, we have the following error event:

$$\mathcal{E}_{\mathsf{U},3} := \{b \in \mathcal{B}_{\text{detect}} | b \notin \mathcal{B}_{\text{URLLC}}\}, \tag{32}$$

which indicates a false-alarm event. More specifically, $\mathcal{E}_{\mathsf{U},3}$ happens when the UE incorrectly declares the detection of a

URLLC message in a block with no URLLC. The URLLC decoding error probability thus is bounded as

$$\epsilon_{b,\mathsf{U}} \leq P_{b-1,\mathsf{D}} \left(\mathbb{P}[\mathcal{E}_{\mathsf{U},1}] + \mathbb{P}[\mathcal{E}_{\mathsf{U},2}]\right) + (1 - P_{b-1,\mathsf{D}})\mathbb{P}[\mathcal{E}_{\mathsf{U},3}], \quad (33)$$

where $P_{b-1,\mathsf{D}}$ is the target detection probability in the previous block $b-1$ and is calculated in Lemma 4. In Appendix A, we analyze each error event which results in Lemma 1.

Lemma 1: The average URLLC decoding error probability is upper bounded as

$$\epsilon_{b,\mathsf{U}} \leq P_{b-1,\mathsf{D}} P_{\mathsf{U},1} + (1 - P_{b-1,\mathsf{D}}) P_{\mathsf{U},2} \quad (34)$$

where

$$P_{\mathsf{U},1} := \tilde{\epsilon}_{\mathsf{U},1} + (\tilde{\epsilon}_{\mathsf{U},1})^{M_{\mathsf{U}} M_v} + \tilde{\epsilon}_{\mathsf{U},2}, \quad (35)$$

$$P_{\mathsf{U},2} := 1 - \left(1 - \frac{\tilde{\epsilon}_{\mathsf{U},2}}{M_{\mathsf{U}} M_v}\right)^{M_{\mathsf{U}} M_v}, \quad (36)$$

$$\tilde{\epsilon}_{\mathsf{U},1} := Q\left(\frac{\ell \mathsf{C}_{\mathsf{U}} - \log(M_{\mathsf{U}} M_v) - K_{\mathsf{U}} \log(\ell)}{\sqrt{\ell \mathsf{V}_{\mathsf{U}}}}\right) + \frac{B}{\sqrt{\ell}}, \quad (37)$$

$$\tilde{\epsilon}_{\mathsf{U},2} := \frac{2}{\ell^{K_{\mathsf{U}}}} \left(\frac{\log 2}{\sqrt{2\pi\ell}} + \frac{2B}{\sqrt{\ell}}\right), \quad (38)$$

for some $K_{\mathsf{U}} > 0$ and $B > 0$ and where $Q(x) = \frac{1}{\sqrt{2\pi}} \int_x^\infty \exp\left(-\frac{t^2}{2}\right) dt$ is the Q-function and

$$\mathsf{C}_{\mathsf{U}} := \sum_{j=1}^{q} \mathsf{C}(\Omega_{b,j}), \quad \mathsf{V}_{\mathsf{U}} := \sum_{j=1}^{q} \mathsf{V}(\Omega_{b,j}), \quad (39)$$

with $\mathsf{C}(x) = \frac{1}{2}\log(1+x)$, $\mathsf{V}(x) := \frac{x(2+x)}{2(1+x)^2}$ with

$$\Omega_{b,j} := \frac{\sigma^2_{y,j} - \sigma^2_{y|v,j}}{\sigma^2_{y|v,j}}, \quad (40)$$

$$\sigma^2_{y,j} := 1 + \lambda_{b,j}\mathsf{P}, \quad (41)$$

$$\sigma^2_{y|v,j} := 1 + \lambda_{b,j}(1 - \alpha_u^2)(1 - \beta_u)\mathsf{P}. \quad (42)$$

Proof: See Appendix A. ∎

Remark 1: Under the assumption that $\mathbb{P}[\mathcal{E}_{\mathsf{U},1}] \to 0$ and $\mathbb{P}[\mathcal{E}_{\mathsf{U},3}] \to 0$, i.e., when the probability that all the URLLC messages are detected correctly is almost 1, then for sufficiently large ℓ,

$$\epsilon_{b,\mathsf{U}} \leq P_{b-1,\mathsf{D}}(\tilde{\epsilon}_{\mathsf{U},1} + \tilde{\epsilon}_{\mathsf{U},2}) = P_{b-1,\mathsf{D}} Q\left(\frac{\ell \mathsf{C}_{\mathsf{U}} - \log(M_{\mathsf{U}} M_v) - O(\log(\ell))}{\sqrt{\ell \mathsf{V}_{\mathsf{U}}}}\right), \quad (43)$$

where C_{U} and V_{U} are defined in (39). This result is consistent with the FBL analysis of decoding error probability of parallel AWGN channels proposed in [34, Theorem 78].

Remark 2: In the single-input single-output (SISO) case, the bound on the URLLC decoding error probability can be recovered from Lemma 1 by setting $q = 1$ and replacing $\lambda_{b,j}$ with λ_b for all $j \in [q]$. In this case, under the assumptions of Remark 1, we have

$$\epsilon_{b,\mathsf{U}} \leq P_{b-1,\mathsf{D}} Q\left(\frac{\ell \mathsf{C}(\Omega_{b,j}) - \log(M_{\mathsf{U}} M_v) - O(\log(\ell))}{\sqrt{\ell \mathsf{V}(\Omega_{b,j})}}\right), \quad (44)$$

where $\mathsf{C}(x) = \frac{1}{2}\log(1+x)$, $\mathsf{V}(x) := \frac{x(2+x)}{2(1+x)^2}$. This result is consistent with the FBL analysis of decoding error probability of point-to-point single AWGN channels proposed by Polyanskiy, Poor and Verdú in [35, Theorem 54].

B. eMBB Transmission Rate Analysis Under the TIN Approach

The eMBB message is decoded at the end of the entire n channel uses. Under this approach, the UE treats URLLC transmissions as noise. Therefore, the decoding of the eMBB message depends on the detection of URLLC messages sent over the η blocks. We have the following two eMBB decoding error events:

$$\mathcal{E}_{\mathsf{e},1} := \{\mathcal{B}_{\text{detect}} \neq \mathcal{B}_{\text{URLLC}}\}, \quad (45)$$

$$\mathcal{E}_{\mathsf{e},2} := \{\hat{m}_{\mathsf{e}} \neq m_e | \mathcal{B}_{\text{detect}} = \mathcal{B}_{\text{URLLC}}\}, \quad (46)$$

where $\mathcal{E}_{\mathsf{e},1}$ happens when the UE does not successfully detect all the transmitted URLLC messages, and $\mathcal{E}_{\mathsf{e},2}$ happens when the UE successfully detects all the transmitted URLLC messages but the decoded eMBB messages does not match the transmitted one.

Recall the definition of B_{dt} as the realization of the set $\mathcal{B}_{\text{detect}}$. The average eMBB decoding error probability is bounded by

$$\epsilon^{(n)}_{\mathsf{e},\text{TIN}} \leq \sum_{B_{\text{dt}}} \mathbb{P}[\mathcal{B}_{\text{detect}} = B_{\text{dt}}] \left(\mathbb{P}[\mathcal{E}_{\mathsf{e},1} | \mathcal{B}_{\text{detect}} = B_{\text{dt}}] + \mathbb{P}[\mathcal{E}_{\mathsf{e},2} | \mathcal{B}_{\text{detect}} = B_{\text{dt}}]\right). \quad (47)$$

In Appendix B, by analyzing the occurrence probability of each error event, we calculate the right-hand side (RHS) of (47). We then use the Berry-Esseen central limit theorem (CLT) for functions [33, Proposition 1] to upper bound the eMBB transmission rate which results in the following lemma.

Lemma 2: Under the TIN approach, the eMBB transmission rate $\mathsf{R}_{\mathsf{e}} := \frac{\log M_{\mathsf{e}}}{n}$ is upper bounded as

$$\mathsf{R}_{\mathsf{e}} \leq \mathsf{C}_{\mathsf{e}} - \sqrt{\frac{\mathsf{V}_{\mathsf{e}}}{n}} Q^{-1}(\epsilon_{\mathsf{e}} - \Delta_{\mathsf{e}}) - K_{\mathsf{e}} \frac{\log(n)}{n} - \frac{\log(M_{\mathsf{s}})}{n} \quad (48)$$

for some $K_{\mathsf{e}} > 0$ and where

$$\mathsf{C}_{\mathsf{e}} := \sum_{B_{\text{dt}}} \mathsf{P}_{\text{dt}}^{|B_{\text{dt}}|} (1 - \mathsf{P}_{\text{dt}})^{\eta - |B_{\text{dt}}|} \tilde{\mathsf{C}}_{\mathsf{e}}, \quad (49)$$

$$\mathsf{V}_{\mathsf{e}} := \sum_{B_{\text{dt}}} \mathsf{P}_{\text{dt}}^{|B_{\text{dt}}|} (1 - \mathsf{P}_{\text{dt}})^{\eta - |B_{\text{dt}}|} \tilde{\mathsf{V}}_{\mathsf{e}}, \quad (50)$$

$$\tilde{\mathsf{C}}_{\mathsf{e}} := \frac{1}{\eta} \sum_{j=1}^{q} \left(\sum_{b \notin B_{\text{dt}}} \mathsf{C}(\Omega^{(1)}_{b,j}) + \sum_{b \in B_{\text{dt}}} \mathsf{C}(\Omega^{(2)}_{b,j})\right), \quad (51)$$

$$\tilde{\mathsf{V}}_{\mathsf{e}} := \frac{1}{\eta} \sum_{j=1}^{q} \left(\sum_{b \notin B_{\text{dt}}} \mathsf{V}(\Omega^{(1)}_{b,j}) + \sum_{b \in B_{\text{dt}}} \mathsf{V}(\Omega^{(2)}_{b,j})\right), \quad (52)$$

where $\mathsf{C}(x) = \frac{1}{2}\log(1+x)$, $\mathsf{V}(x) := \frac{x(2+x)}{2(1+x)^2}$,

$$\mathsf{P}_{\text{dt}} := P_{b-1,\mathsf{D}}(1 - (\hat{\epsilon}_{\mathsf{U},1})^{M_{\mathsf{U}} M_v}) + (1 - P_{b-1,\mathsf{D}}) P_{\mathsf{U},2}, \quad (53)$$

$$\Delta_{\mathsf{e}} := 1 + \frac{\tilde{B}}{\sqrt{n}} \left(1 + \frac{4}{n^{K_{\mathsf{e}}}}\right) + \frac{2\log 2}{n^{K_{\mathsf{e}}}\sqrt{2n\pi}}$$

$$- \sum_{B_{\mathsf{dt}}} \left(P_{b-1,\mathsf{D}}(1-(\tilde{\epsilon}_{\mathsf{U},1})^{M_{\mathsf{U}}M_v})\right)^{|B_{\mathsf{dt}}|} \times \left((1-P_{b-1,\mathsf{D}})(1-P_{\mathsf{U},2})\right)^{\eta-|B_{\mathsf{dt}}|}, \quad (54)$$

$$\Omega_{b,j}^{(1)} := \frac{\sigma_{y,j}^2 - \sigma_{y|s^{(1)},j}^2}{\sigma_{y|s^{(1)},j}^2}, \quad \Omega_{b,j}^{(2)} := \frac{\sigma_{y,j}^2 - \sigma_{y|s^{(2)},j}^2}{\sigma_{y|s^{(2)},j}^2}, \quad (55)$$

with $\hat{\epsilon}_{\mathsf{U},1} := \tilde{\epsilon}_{\mathsf{U},1} - \frac{2\tilde{B}}{\sqrt{\ell}}$, and where $\tilde{\epsilon}_{\mathsf{U},1}$ and $\tilde{\epsilon}_{\mathsf{U},2}$ are defined in (37) and (38), respectively, and

$$\sigma_{y|s^{(1)},j}^2 := 1 + \lambda_{b,j}(1-\alpha_{s,1}^2)(1-\beta_{s,1})\mathsf{P}, \quad (56)$$

$$\sigma_{y|s^{(2)},j}^2 := 1 + \lambda_{b,j}\mathsf{P}\Big(1-(1-\alpha_u)^2(1-\beta_u) (1-(1-\alpha_{s,2}^2)(1-\beta_{s,2}))\Big). \quad (57)$$

Proof: See Appendix B. ∎

Remark 3: The parameter P_{dt} can be interpreted as the probability of correct detection of a URLLC message in a given block b. In the case where $\lambda_{b,j} = \lambda$ for all $b \in [\eta]$ and all $j \in [q]$, the capacity and the channel dispersion terms can be simplified as

$$\mathsf{C}_{\mathsf{e}} = q\left((1-\mathsf{P}_{\mathsf{dt}})\mathsf{C}(\Omega^{(1)}) + \mathsf{P}_{\mathsf{dt}}\mathsf{C}(\Omega^{(2)})\right), \quad (58)$$

$$\mathsf{V}_{\mathsf{e}} = q\left((1-\mathsf{P}_{\mathsf{dt}})\mathsf{V}(\Omega^{(1)}) + \mathsf{P}_{\mathsf{dt}}\mathsf{V}(\Omega^{(2)})\right), \quad (59)$$

where $\Omega^{(1)}$ and $\Omega^{(2)}$ are obtained from (55) by replacing $\lambda_{b,j}$ with λ. As a result, under the TIN approach, the eMBB transmission channel is interpreted as q parallel AWGN channels where in each channel, with probability P_{dt} a URLLC message is detected and with probability $1-P_{\mathsf{dt}}$, no URLLC message is detected.

C. eMBB Transmission Rate Analysis Under the SIC Approach

Under this approach, before decoding the eMBB message, the UE first mitigates the interference of correctly decoded URLLC messages over the η blocks. Therefore, the decoding of the eMBB message depends on both the detection of URLLC messages sent over η blocks and the correct decoding of such messages. Recall the definition of B_{dt} as a realization of the set $\mathcal{B}_{\text{detect}}$ and the definition of B_{dc} as a realization of the set $\mathcal{B}_{\text{decode}}$. To decode the eMBB message, we again have the two error events defined in (45) and (46). The average eMBB decoding error probability is bounded as

$$\epsilon_{\mathsf{e,SIC}}^{(n)} \leq \sum_{B_{\mathsf{dt}}} \mathbb{P}[\mathcal{B}_{\text{detect}} = B_{\mathsf{dt}}]\Big(\mathbb{P}[\mathcal{E}_{\mathsf{e},1}|\mathcal{B}_{\text{detect}} = B_{\mathsf{dt}}] + \sum_{B_{\mathsf{dc}}} \mathbb{P}[\mathcal{B}_{\text{decode}} = B_{\mathsf{dc}}|\mathcal{B}_{\text{detect}} = \mathcal{B}_{\text{URLLC}}, \mathcal{B}_{\text{detect}} = B_{\mathsf{dt}}] \mathbb{P}[\mathcal{E}_{\mathsf{e},2}|\mathcal{B}_{\text{detect}} = B_{\mathsf{dt}}, \mathcal{B}_{\text{decode}} = B_{\mathsf{dc}}]\Big). \quad (60)$$

Note that, compared to the TIN approach, here the decoding of the eMBB message not only depends on the detected URLLC messages set B_{dt} but also depends on the correctly decoded URLLC messages set $B_{\mathsf{dc}} \subset B_{\mathsf{dt}}$. Under this approach, we have the following lemma on the eMBB transmission rate.

Lemma 3: Under the SIC approach, the eMBB transmission rate $\mathsf{R}_{\mathsf{e}} := \frac{\log M_{\mathsf{e}}}{n}$ is upper bounded by

$$\mathsf{R}_{\mathsf{e}} \leq \mathsf{C}_{\mathsf{e},2} - \sqrt{\frac{\mathsf{V}_{\mathsf{e},2}}{n}}Q^{-1}(\epsilon_{\mathsf{e}} - \Delta_{\mathsf{e}}) - K_{\mathsf{e}}\frac{\log(n)}{n} - \frac{\log(M_{\mathsf{s}})}{n} \quad (61)$$

for some $K_{\mathsf{e}} > 0$ and where

$$\mathsf{C}_{\mathsf{e},2} := \sum_{B_{\mathsf{dt}}}\sum_{B_{\mathsf{dc}}} \mathcal{A}(\mathsf{P}_{\mathsf{dt}}, \mathsf{P}_{\mathsf{dc}})\tilde{\mathsf{C}}_{\mathsf{e},2}, \quad (62)$$

$$\mathsf{V}_{\mathsf{e},2} := \sum_{B_{\mathsf{dt}}}\sum_{B_{\mathsf{dc}}} \mathcal{A}(\mathsf{P}_{\mathsf{dt}}, \mathsf{P}_{\mathsf{dc}})\tilde{\mathsf{V}}_{\mathsf{e},2}, \quad (63)$$

$$\tilde{\mathsf{C}}_{\mathsf{e},2} := \frac{1}{\eta}\sum_{j=1}^{q}\left(\sum_{b\notin B_{\mathsf{dt}}}\mathsf{C}(\Omega_{b,j}^{(1)}) + \sum_{b\in B_{\mathsf{dt}}\setminus B_{\mathsf{dc}}}\mathsf{C}(\Omega_{b,j}^{(2)}) + \sum_{b\in B_{\mathsf{dc}}}\mathsf{C}(\Omega_{b,j}^{(3)})\right), \quad (64)$$

$$\tilde{\mathsf{V}}_{\mathsf{e},2} := \frac{1}{\eta}\sum_{j=1}^{q}\left(\sum_{b\notin B_{\mathsf{dt}}}\mathsf{V}(\Omega_{b,j}^{(1)}) + \sum_{b\in B_{\mathsf{dt}}\setminus B_{\mathsf{dc}}}\mathsf{V}(\Omega_{b,j}^{(2)}) + \sum_{b\in B_{\mathsf{dc}}}\mathsf{V}(\Omega_{b,j}^{(3)})\right), \quad (65)$$

where $\mathsf{C}(x) = \frac{1}{2}\log(1+x)$, $\mathsf{V}(x) := \frac{x(2+x)}{2(1+x)^2}$,

$$\mathcal{A}(a,b) := a^{|B_{\mathsf{dt}}|}(1-a)^{\eta-|B_{\mathsf{dt}}|}b^{|B_{\mathsf{dc}}|}(1-b)^{|B_{\mathsf{dt}}|-|B_{\mathsf{dc}}|}, \quad (66)$$

and

$$\mathsf{P}_{\mathsf{dc}} := 1 - \tilde{\epsilon}_{\mathsf{U},1} - \tilde{\epsilon}_{\mathsf{U},2}, \quad (67)$$

$$\Omega_{b,j}^{(3)} := \frac{\sigma_{y|v,j}^2 - \sigma_{y|s^{(2)}v,j}^2}{\sigma_{y|s^{(2)}v,j}^2} \quad (68)$$

with

$$\sigma_{y|s^{(2)}v,j}^2 := 1 + \lambda_{b,j}(1-\alpha_u)^2(1-\alpha_{s,1})^2(1-\beta_u)(1-\beta_{s,1})\mathsf{P}, \quad (69)$$

and $\tilde{\epsilon}_{\mathsf{U},1}$ and $\tilde{\epsilon}_{\mathsf{U},2}$ are defined in (37) and (38), respectively.

Proof: See Appendix C. ∎

Remark 4: In Lemma 3, P_{dc} can be interpreted as the probability of correctly decoding a URLLC message in each block b. In the case where $\lambda_{b,j} = \lambda$ for all $b \in [\eta]$ and all $j \in [q]$, the capacity and the channel dispersion terms can be simplified as

$$\mathsf{C}_{\mathsf{e},2} = q(1-P_{\mathsf{dt}})\mathsf{C}(\Omega^{(1)}) + qP_{\mathsf{dt}}\left((1-P_{\mathsf{dc}})\mathsf{C}(\Omega^{(2)}) + P_{\mathsf{dc}}\mathsf{C}(\Omega^{(3)})\right), \quad (70)$$

$$\mathsf{V}_{\mathsf{e},2} = q(1-P_{\mathsf{dt}})\mathsf{V}(\Omega^{(1)}) + qP_{\mathsf{dt}}\left((1-P_{\mathsf{dc}})\mathsf{V}(\Omega^{(2)}) + P_{\mathsf{dc}}\mathsf{V}(\Omega^{(3)})\right), \quad (71)$$

where $\Omega^{(1)}$, $\Omega^{(2)}$ and $\Omega^{(3)}$ are obtained from (55) and (68) by replacing $\lambda_{b,j}$ with λ. As a result, under the SIC approach, the eMBB transmission channel is interpreted as q parallel AWGN channels where in each channel, with probability $1-P_{\mathsf{dt}}$, no URLLC message is detected, with probability $P_{\mathsf{dt}}P_{\mathsf{dc}}$ a URLLC message is correctly detected and decoded, and with probability $P_{\mathsf{dt}}(1-P_{\mathsf{dc}})$ the correctly detected URLLC message is missed decoded.

D. Target Detection Probability Analysis

Given that the sensing channel state is known at the SR, the MIMO channel in (2) is transferred into the following set of q parallel channels

$$\boldsymbol{Y}_{b,s,j} = \boldsymbol{X}_{b,j}\sqrt{\gamma_{b,j}} + \boldsymbol{N}_{b,s,j}, \tag{72}$$

for each $j \in [q]$ and each $b \in [\eta]$. Here, $\gamma_{b,1} \geq \gamma_{b,2} \geq \ldots \geq \gamma_{b,q}$ are the q largest eigenvalues of $\mathbf{H}_{b,s}^H \mathbf{H}_{b,s}$. The LRT test in each block $b \in [\eta]$ is defined in (3). Given that $\boldsymbol{N}_{b,s,j} \sim \mathcal{N}(0, \mathbf{I}_{\ell\times\ell})$, thus $f\left(\boldsymbol{Y}_{b,s,j}|\mathcal{H}_1\right)$ is a Gaussian distribution. However, due to our power-shell code construction, this is not the case for $f\left(\boldsymbol{Y}_{b,s,j}|\mathcal{H}_1\right)$. Hence, we take a change of metric measurement approach by introducing the following new LRT test:

$$\tilde{T}_b := \log\left(\prod_{j=1}^{q} \frac{Q\left(\boldsymbol{Y}_{b,s,j}|\mathcal{H}_1\right)}{f\left(\boldsymbol{Y}_{b,s,j}|\mathcal{H}_0\right)}\right) \underset{\mathcal{H}_0}{\overset{\mathcal{H}_1}{\gtrless}} \delta, \tag{73}$$

where $Q\left(\boldsymbol{Y}_{b,s,j}|\mathcal{H}_1\right)$ is a Gaussian distribution and $\boldsymbol{y}_{b,s,j}|\mathcal{H}_1 \sim \mathcal{N}(\boldsymbol{\mu}_{b,j}, \sigma_{b,j}^2 \boldsymbol{I}_\ell)$ with

$$\boldsymbol{\mu}_{b,j} := \begin{cases} \sqrt{\gamma_{b,j}}(1-\alpha_{s,1})\boldsymbol{x}_{b,j}^{(\mathsf{s},1)}, & b \notin \mathcal{B}_{\text{URLLC}} \\ \sqrt{\gamma_{b,j}}(1-\alpha_u)(1-\alpha_{s,2})\boldsymbol{x}_{b,j}^{(\mathsf{s},2)}, & \text{o.w.} \end{cases} \tag{74}$$

$$\sigma_{b,j}^2 := 1 + \gamma_{b,j}\kappa_2(1-\kappa_1)\mathsf{P} \tag{75}$$

where

$$\kappa_1 := \begin{cases} (1-\alpha_{s,1}^2)(1-\beta_{s,1}), & b \notin \mathcal{B}_{\text{URLLC}} \\ (1-\alpha_{s,2}^2)(1-\beta_{s,2}), & \text{o.w.} \end{cases} \tag{76}$$

$$\kappa_2 := \begin{cases} 1, & b \notin \mathcal{B}_{\text{URLLC}} \\ (1-\beta_u)(1-\alpha_u)^2, & \text{o.w.} \end{cases} \tag{77}$$

The test thus can be written as

$$\tilde{T}_b = \sum_{j=1}^{q}\left(||\boldsymbol{Y}_{b,s,j}||^2 - \frac{||\boldsymbol{Y}_{b,s,j} - \boldsymbol{\mu}_{b,j}||^2}{\sigma_{b,j}^2}\right) \underset{\mathcal{H}_0}{\overset{\mathcal{H}_1}{\gtrless}} \delta. \tag{78}$$

Accordingly, in each block b, the target detection and false alarm probabilities are given by

$$P_{b,\mathsf{D}} = \mathbb{P}[\tilde{T}_b > \delta|\mathcal{H}_1], \quad P_{b,\text{FA}} = \mathbb{P}[\tilde{T}_b > \delta|\mathcal{H}_0]. \tag{79}$$

We set δ such that $P_{b,\text{FA}} = P_{\text{FA}}$ across all η blocks. The target detection probability then is given by the following lemma.

Lemma 4: The target detection probability is given by

$$P_{b,\mathsf{D}} = 1 - F_{\tilde{\chi}_2}\left(F_{\tilde{\chi}_1}^{-1}(1-P_{\text{FA}})\right), \tag{80}$$

where P_{FA} is the desired false alarm probability, $\tilde{\chi}_1(\{w_{b,j}\}_{j=1}^q, \ell, \{\nu_{b,j}\}_{j=1}^q)$ and $\tilde{\chi}_2(\{w_{b,j}\}_{j=1}^q, \ell, \{\tilde{\nu}_{b,j}\}_{j=1}^q)$ are generalized chi-square distributions with $F_{\tilde{\chi}_1}(\cdot)$ and $F_{\tilde{\chi}_2}(\cdot)$ as their corresponding cumulative distribution functions (CDFs) and

$$w_{b,j} := 1 - \frac{1}{\sigma_{b,j}^2}, \tag{81a}$$

$$\nu_{b,j} := \kappa_1\kappa_2\ell\mathsf{P}\left(\frac{1-w_{b,j}}{w_{b,j}}\right)^2, \tag{81b}$$

$$\tilde{\nu}_{b,j} := \begin{cases} \gamma_{b,j}\ell\mathsf{P}\tau_2(\beta_{s,1},\alpha_{s,1}) & b \notin \mathcal{B}_{\text{URLLC}}, \\ \gamma_{b,j}\ell\mathsf{P}\tau_3 & \text{o.w.} \end{cases} \tag{81c}$$

where

$$\tau_2(b,a) := b + (1-b)\left(a + \frac{\sigma_{b,j}^2}{\sigma_{b,j}^2 - 1}(1-a)\right)^2, \tag{82}$$

$$\tau_3 := \beta_u + (1-\beta_u)(\alpha_u^2 + (1-\alpha_u)^2\tau(\beta_{s,2},\alpha_{s,2})), \tag{83}$$

and $\sigma_{b,j}^2$, κ_1 and κ_2 are defined in (75), (76) and (77), respectively.

Proof: See Appendix D. ∎

Remark 5: In the SISO case, the target detection probability can be recovered from Lemma 4. In this case, $\tilde{\chi}_1$ and $\tilde{\chi}_2$ are non-central chi-square distributions with degree of ℓ and parameters ν_b and $\tilde{\nu}_b$, respectively. These parameters can be calculated from (81) by assuming $\gamma_{b,j} = \gamma_b$ for all $j \in [q]$.

E. Rate-Reliability-Detection Trade-off

By combining Lemmas 1, 2 and 4 with Proposition 1, we have the following theorem on the rate-reliability-detection trade-off under the TIN approach.

Theorem 1: Given n and P, the rate-reliability-detection trade-off under the TIN approach is given by

$$\max_{\boldsymbol{\beta},\boldsymbol{\alpha}} \mathsf{C}_\mathsf{e} - \sqrt{\frac{\mathsf{V}_\mathsf{e}}{n}}Q^{-1}(\epsilon_\mathsf{e} - \Delta_\mathsf{e}) - K_\mathsf{e}\frac{\log(n)}{n} - \frac{\log(M_\mathsf{s})}{n} \tag{84a}$$

$$\text{s.t.: } P_{b-1,\mathsf{D}}P_{\mathsf{U},1} + (1-P_{b-1,\mathsf{D}})P_{\mathsf{U},2} \leq \epsilon_\mathsf{U}, \quad \forall b \in [\eta], \tag{84b}$$

$$1 - F_{\tilde{\mathcal{X}}_2}(F_{\tilde{\mathcal{X}}_1}^{-1}(1-P_{\text{FA}})) \geq \mathsf{P}_\mathsf{D}, \quad \forall b \in [\eta], \tag{84c}$$

where $\boldsymbol{\beta} := \{\beta_u, \beta_{s,1}, \beta_{s,2}\}$ and $\boldsymbol{\alpha} := \{\alpha_u, \alpha_{s,1}, \alpha_{s,2}\}$.

By combining Lemmas 1, 3, and 4 with Proposition 1, we have the following theorem on the rate-reliability-detection trade-off under the SIC approach.

Theorem 2: Given n and P, the rate-reliability-detection trade-off under the SIC approach is given by

$$\max_{\boldsymbol{\beta},\boldsymbol{\alpha}} \mathsf{C}_{\mathsf{e},2} - \sqrt{\frac{\mathsf{V}_{\mathsf{e},2}}{n}}Q^{-1}(\epsilon_\mathsf{e} - \Delta_{\mathsf{e},2}) - K_{\mathsf{e},2}\frac{\log(n)}{n} - \frac{\log(M_\mathsf{s})}{n} \tag{85a}$$

$$\text{s.t.: (84b) and (84c)} \tag{85b}$$

where $\boldsymbol{\beta} := \{\beta_u, \beta_{s,1}, \beta_{s,2}\}$ and $\boldsymbol{\alpha} := \{\alpha_u, \alpha_{s,1}, \alpha_{s,2}\}$.

V. Numerical Analysis

In this section, we numerically evaluate the rate-reliability-detection trade-off of Theorem 1 and Theorem 2. For given $\mathsf{P}, n, \eta, P_{\text{FA}}, \epsilon_\mathsf{e}$ and ϵ_U, we first find values of α_u and β_u such that $\epsilon_{b,\mathsf{U}}$ is below ϵ_U in all blocks. Meaning that the constraint (84b) is satisfied for all blocks. Next, we maximize the upper bound on the eMBB rate in (84a) over $\beta_{s,1}, \beta_{s,2}, \alpha_{s,1}, \alpha_{s,2}$ while satisfying the minimum required target detection probability (i.e., P_D) over all blocks.

We compare our results with the following two baseline schemes:

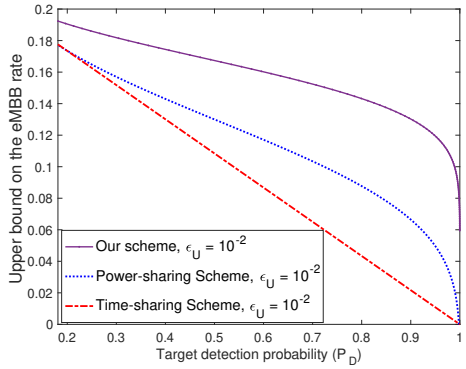

Fig. 2: Comparing our DPC-based scheme under the TIN approach with power-sharing and time-sharing schemes for $\mathsf{P} = 0.5$, $\ell = 150$, $\eta = 10$, $P_{FA} = 10^{-6}$, $\epsilon_e = 10^{-3}$.

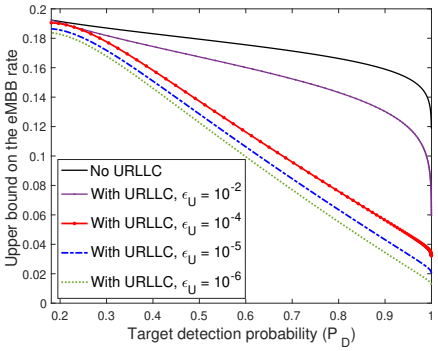

Fig. 3: Our scheme under the TIN approach with different values of the URLLC decoding error probability threshold for $\mathsf{P} = 0.5$, $\ell = 150$, $\eta = 10$, $P_{FA} = 10^{-6}$, $\epsilon_e = 10^{-3}$.

- *Power-sharing scheme*: under this scheme, sensing and communication signals are superposed by simply adding the two corresponding codewords [27]. We can obtain the power-sharing scheme from the proposed DPC-based scheme by setting $\alpha_u = \alpha_{s,1} = \alpha_{s,2} = 0$. We then share the total transmit power P between the communication and sensing tasks using the power sharing parameters $\beta_{s,1}, \beta_u$ and $\beta_{s,2}$ as explained in our scheme.
- *Time-sharing scheme*: under this scheme, the available transmission block is shared between the sensing and communication tasks and thus the two tasks are performed separately [19]. To analyze the performance of this scheme, in each block $b \notin \mathcal{B}_{\text{URLLC}}$, we share the ℓ channel uses between the communication task of transmitting the eMBB message and the sensing task. In each block $b \in \mathcal{B}_{\text{URLLC}}$, we share the ℓ channel uses among the communication task of transmitting a URLLC message, transmitting the eMBB message and the sensing task. Each individual task is performed using the transmit power P.

Fig. 2 illustrates the upper bound on the eMBB transmission rate as a function of P_{D} for our DPC-based scheme under the TIN approach. We compare the result with the power-sharing and time-sharing schemes when ϵ_{U} is fixed at 10^{-2}. As can be seen from this figure, our scheme significantly outperforms the other two schemes. Fig. 3 illustrates the upper bound on the eMBB transmission rate as a function of P_{D} for our proposed TIN scheme under different levels of URLLC reliability. It can be seen that as we decrease the required threshold on the URLLC decoding error probability (i.e., ϵ_{U}) the eMBB rate decreases. In other words, increasing URLLC reliability requirements decreases the eMBB transmission rate.

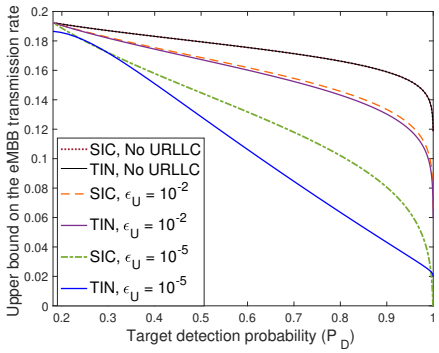

Fig. 4: Comparing the upper bound on the eMBB transmission rate under the TIN and SIC approaches for ϵ_{U} set at 10^{-2} and 10^{-5} and $\mathsf{P} = 0.5$, $\ell = 150$, $\eta = 10$, $P_{FA} = 10^{-6}$, $\epsilon_e = 10^{-3}$.

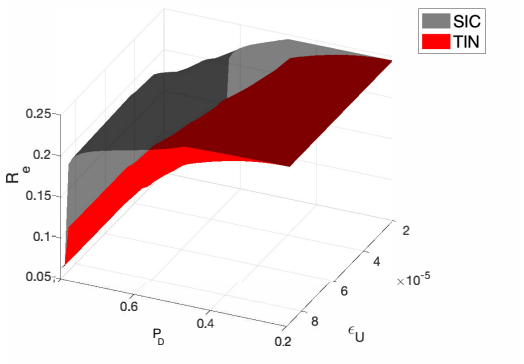

Fig. 5: An illustration of the upper bound on the eMBB transmission as a function of P_{D} and ϵ_{U} under the TIN and SIC approaches. In this figure, ϵ_{U} varies from 10^{-5} to 10^{-4} with a step size of 10^{-5}. In this figure, $\mathsf{P} = 0.5$, $\ell = 150$, $\eta = 10$, $P_{\text{FA}} = 10^{-4}$ and $\epsilon_{\mathsf{e}} = 10^{-2}$.

Next we compare the performance of our DPC-based scheme under the TIN and the SIC approaches. In Fig 4, we plot the upper bound on the eMBB transmission rate R_{e} under both approaches for different values of ϵ_{U}. It can be seen that in the case of no URLLC or when the URLLC reliability constraint is very low, i.e., $\epsilon_{\mathsf{U}} = 10^{-2}$, the TIN and the SIC approaches have similar performance. However, at high URLLC requirements, the SIC approach outperforms the TIN. Fig. 5 illustrates the upper bound on the eMBB transmission as a function of P_{D} and ϵ_{U} for both the TIN and SIC approaches. In this plot, ϵ_{U} varies from 10^{-5} to 10^{-4} with a step size of 10^{-5} which implies high requirements on the URLLC reliability and results in the outperformance of the SIC over the TIN. However, the performance gap decreases when the target detection probability, i.e., P_{D}, is either very low or very high. Specifically, when

the target detection probability is very low, most blocks are with no URLLC, resulting in comparable performance for both approaches. At high target detection probability, most blocks are with URLLC and thus more subtracted URLLC interference will be wrong which introduces error in the eMBB decoding under the SIC and eventually reduces the gap between the two approaches.

VI. Conclusion

We have proposed a MIMO ISAC-enabled URLLC system where a BS communicates with a UE and a SR collects echo signals reflected from a target of interest. The BS simultaneously transmit messages from eMBB and URLLC services. During each eMBB transmission, the transmission of an additional URLLC message is triggered when the SR sensed the presence of the target. To reinforce URLLC transmissions, the interference of both eMBB and sensing signals were mitigated using DPC. For this system, we formulated the rate-reliability-detection trade-off in the finite blocklength regime. Our numerical analysis shows a significant outperformance of our scheme over the power-sharing and the time-sharing methods.

Appendix A
Proof of Lemma 1

Recall that all the codewords are uniformly distributed on the power shell. As a result of this code construction, our input codewords are non i.i.d. We thus take a change of metric approach and instead of the information density metric $i_b^{(\mathsf{U})}(\mathbf{V}_b;\mathbf{Y}_{b,c})$ defined in (21), we use the following metric:

$$\tilde{i}_b^{(\mathsf{U})}(\mathbf{V}_b;\mathbf{Y}_{b,c})=\sum_{j=1}^{q}\log\frac{Q_{\boldsymbol{Y}_{b,c,j}|\boldsymbol{V}_{b,j}}(\mathbf{y}_{b,c}|\mathbf{v}_b)}{Q_{\mathbf{Y}_{b,c}}(\mathbf{y}_{b,c})}, \tag{86}$$

where Q's are i.i.d Gaussian distributions. Specifically,

$$Q_{\boldsymbol{Y}_{b,c,j}}\sim\mathcal{N}\left(\boldsymbol{y}_{b,c,j}:\mathbf{0},\sigma_{y,j}^2\mathbf{I}_{\ell\times\ell}\right), \tag{87}$$

$$Q_{\boldsymbol{Y}_{b,c,j}|\boldsymbol{V}_{b,j}}\sim\mathcal{N}\left(\boldsymbol{y}_{b,c,j}:\sqrt{\lambda_{b,j}}\boldsymbol{v}_{b,j},\sigma_{y|v,j}^2\mathbf{I}_{\ell\times\ell}\right), \tag{88}$$

where $\sigma_{y,j}^2$ and $\sigma_{y|v,j}^2$ are defined in (41) and (42), respectively. The following lemma shows that the random variable $\tilde{i}_b^{(\mathsf{U})}(\mathbf{V}_b;\mathbf{Y}_{b,c})$ converges in distribution to a Gaussian distribution.

Lemma 5: The following holds:

$$\tilde{i}_b^{(\mathsf{U})}(\mathbf{V}_b;\mathbf{Y}_{b,c})\sim\mathcal{N}(\ell\mathsf{C}_\mathsf{U},\ell\mathsf{V}_\mathsf{U}), \tag{89}$$

where

$$\mathsf{C}_\mathsf{U}:=\sum_{j=1}^{q}\mathsf{C}(\Omega_{b,j}),\quad \mathsf{V}_\mathsf{U}:=\sum_{j=1}^{q}\mathsf{V}(\Omega_{b,j}) \tag{90}$$

with $\mathsf{C}(x)=\frac{1}{2}\log(1+x)$, $\mathsf{V}(x):=\frac{x(2+x)}{2(1+x)^2}$ and $\Omega_{b,j}$ is defined in (40).

Proof: See Appendix E. ∎

We are now ready to analyze the URLLC decoding error probability. Recall the bound on the average URLLC decoding error probability from (33). Recall the definition of $\mathcal{E}_{\mathsf{U},1}$, $\mathcal{E}_{\mathsf{U},2}$ and $\mathcal{E}_{\mathsf{U},3}$ from (30), (31) and (32), respectively.

1) Analyzing $\mathbb{P}[\mathcal{E}_{\mathsf{U},1}]$: This is equivalent to the probability that for all $v\in[M_v]$ and for all $m\in[M_\mathsf{U}]$ there is no codeword $\mathbf{V}_b(m,v)$ such that $\tilde{i}_b^{(\mathsf{U})}(\mathbf{V}_b;\mathbf{Y}_{b,c})>\delta_\mathsf{U}$. Hence,

$$\mathbb{P}[\mathcal{E}_{\mathsf{U},1}]=\left(\mathbb{P}[\tilde{i}_b^{(\mathsf{U})}(\mathbf{V}_b;\mathbf{Y}_{b,c})\le\delta_\mathsf{U}]\right)^{M_\mathsf{U}M_v}. \tag{91}$$

2) Analyzing $\mathbb{P}[\mathcal{E}_{\mathsf{U},2}]$: This is equivalent to the probability that the UE has detected a URLLC message but the decoded one does not match the transmitted one. To evaluate this probability, we use the threshold bound for maximum-metric decoding. I.e., for any given threshold δ_U:

$$\begin{aligned}\mathbb{P}[\mathcal{E}_{\mathsf{U},2}]\le{}&\mathbb{P}[\tilde{i}_b^{(\mathsf{U})}(\mathbf{V}_b(m_{b,\mathsf{U}},v);\mathbf{Y}_{b,c})\le\delta_\mathsf{U}]\\&+(M_\mathsf{U}M_v-1)\mathbb{P}[\tilde{i}_b^{(\mathsf{U})}(\bar{\mathbf{V}}_b(m',v');\mathbf{Y}_{b,c})>\delta_\mathsf{U}]\end{aligned} \tag{92}$$

where $m'\in[M_\mathsf{U}]$, $v'\in[M_v]$ and $(m_{b,\mathsf{U}},v)\neq(m',v')$ and $\bar{\mathbf{V}}_b\sim f_{\mathbf{V}_b}$ and is independent of $\mathbf{V}_b$ and $\mathbf{Y}_{b,c}$.

3) Analyzing $\mathbb{P}[\mathcal{E}_{\mathsf{U},3}]$: This is equivalent to the probability that no URLLC message has been sent over block b but there is at least one codeword $\bar{\mathbf{V}}_b$ such that $\mathbb{P}[\tilde{i}_b^{(\mathsf{U})}(\bar{\mathbf{V}}_b;\mathbf{Y}_{b,c})>\delta_\mathsf{U}]$. Hence,

$$\mathbb{P}[\mathcal{E}_{\mathsf{U},3}]=1-\left(\mathbb{P}[\tilde{i}_b^{(\mathsf{U})}(\bar{\mathbf{V}}_b;\mathbf{Y}_{b,c})\le\delta_\mathsf{U}]\right)^{M_\mathsf{U}M_v}. \tag{93}$$

Combining (33), (91), (92) and (93), we have

$$\begin{aligned}\epsilon_{b,\mathsf{U}}\le{}&P_{b-1,\mathsf{D}}\Big(\mathbb{P}[\tilde{i}_b^{(\mathsf{U})}(\mathbf{V}_b;\mathbf{Y}_{b,c})\le\delta_\mathsf{U}]^{M_\mathsf{U}M_v}\\&+\mathbb{P}[\tilde{i}_b^{(\mathsf{U})}(\mathbf{V}_b;\mathbf{Y}_{b,c})\le\delta_\mathsf{U}]\\&+(M_\mathsf{U}M_v-1)\mathbb{P}[\tilde{i}_b^{(\mathsf{U})}(\bar{\mathbf{V}}_b;\mathbf{Y}_{b,c})>\delta_\mathsf{U}]\Big)\\&+(1-P_{b-1,\mathsf{D}})\left(1-\left(\mathbb{P}[\tilde{i}_b^{(\mathsf{U})}(\bar{\mathbf{V}}_b;\mathbf{Y}_{b,c})\le\delta_\mathsf{U}]\right)^{M_\mathsf{U}M_v}\right).\end{aligned} \tag{94}$$

For some $K_\mathsf{U}>0$, set

$$\delta_\mathsf{U}:=\log(M_\mathsf{U}M_v)+K_\mathsf{U}\log(\ell). \tag{95}$$

To evaluate $\mathbb{P}[i_b^{(\mathsf{U})}(\bar{\mathbf{V}}_b;\mathbf{Y}_{b,c})>\delta_\mathsf{U}]$ we follow [35, Lemma 47] which results in

$$\mathbb{P}[\tilde{i}_b^{(\mathsf{U})}(\bar{\mathbf{V}}_b;\mathbf{Y}_{b,c})>\delta_\mathsf{U}]\le\frac{2}{M_\mathsf{U}M_v\ell^{K_\mathsf{U}}}\left(\frac{\log 2}{\sqrt{2\pi\ell}}+\frac{2B}{\sqrt{\ell}}\right). \tag{96}$$

Given that $\tilde{i}_b^{(\mathsf{U})}(\mathbf{V}_b(m_{b,\mathsf{U}},v);\mathbf{Y}_{b,c})$ follows a Gaussian distribution (as shown in Lemma 5), thus we employ the Berry-Esseen CLT for functions [33, Proposition 1] to bound the following probability:

$$\begin{aligned}&\mathbb{P}[\tilde{i}_b^{(\mathsf{U})}(\mathbf{V}_b;\mathbf{Y}_{b,c})\le\delta_\mathsf{U}]\\&\le Q\left(\frac{-\log(M_\mathsf{U}M_v)+\ell\mathsf{C}_\mathsf{U}-K_\mathsf{U}\log(\ell)}{\sqrt{\ell\mathsf{V}_\mathsf{U}}}\right)+\frac{B}{\sqrt{\ell}},\end{aligned} \tag{97}$$

where $B>0$ is a constant. Combining (96) and (97) with (94) concludes the proof.

Appendix B
Proof of Lemma 2

Recall the average decoding error probability of eMBB under the TIN approach from (47). We now evaluate the right-hand side (RHS) of (47).

1) Analyzing $\mathbb{P}[\mathcal{B}_{detect} = B_{dt}]$:

$$\begin{aligned}\tilde{\mathsf{P}}_{\mathsf{dt}} &:= \mathbb{P}[b \in \mathcal{B}_{\text{URLLC}}]\mathbb{P}[b \in \mathcal{B}_{\text{detect}} | b \in \mathcal{B}_{\text{URLLC}}] \\ &\quad + \mathbb{P}[b \notin \mathcal{B}_{\text{URLLC}}]\mathbb{P}[b \in \mathcal{B}_{\text{detect}} | b \notin \mathcal{B}_{\text{URLLC}}] \quad (98) \\ &= \mathsf{P}_{b-1,\mathsf{D}}(1 - \mathbb{P}[\mathcal{E}_{\text{U},1}]) + (1 - \mathsf{P}_{b-1,\mathsf{D}})\mathbb{P}[\mathcal{E}_{\text{U},3}]. \quad (99)\end{aligned}$$

We thus have

$$\mathbb{P}[\mathcal{B}_{\text{detect}} = B_{\text{dt}}] = \tilde{\mathsf{P}}_{\text{dt}}^{|B_{\text{dt}}|}(1 - \tilde{\mathsf{P}}_{\text{dt}})^{\eta - |B_{\text{dt}}|}, \quad (100)$$

which is equivalent to the probability that the UE detects URLLC messages in all the blocks in B_{dt} and there is no URLLC detection in blocks that are in $[\eta] \backslash B_{\text{dt}}$.

2) Analyzing $\mathbb{P}[\mathcal{E}_{\mathsf{e},1} | \mathcal{B}_{detect} = B_{dt}]$: This error event is equivalent to the probability that the set of blocks in which UE detects URLLC is different from the set of blocks in which the BS transmits URLLC messages (i.e., $\mathcal{B}_{\text{detect}} \neq \mathcal{B}_{\text{URLLC}}$).

$$\begin{aligned}&\mathbb{P}[\mathcal{E}_{\mathsf{e},1} | \mathcal{B}_{\text{detect}} = B_{\text{dt}}] \\ &= \mathbb{P}[\mathcal{B}_{\text{URLLC}} \neq B_{\text{dt}} | \mathcal{B}_{\text{detect}} = B_{\text{dt}}] \quad (101) \\ &= 1 - \frac{\mathbb{P}[\mathcal{B}_{\text{URLLC}} = B_{\text{dt}}]\mathbb{P}[\mathcal{B}_{\text{detect}} = B_{\text{dt}} | \mathcal{B}_{\text{URLLC}} = B_{\text{dt}}]}{\mathbb{P}[\mathcal{B}_{\text{detect}} = B_{\text{dt}}]} \quad (102) \\ &= 1 - \frac{(P_{b-1,\mathsf{D}}(1 - \mathbb{P}[\mathcal{E}_{\text{U},1}]))^{|B_{\text{dt}}|}}{\tilde{\mathsf{P}}_{\text{dt}}^{|B_{\text{dt}}|}} \cdot \\ &\qquad \times \frac{((1 - \mathbb{P}[\mathcal{E}_{\text{U},3}])(1 - P_{b-1,\mathsf{D}}))^{\eta - |B_{\text{dt}}|}}{(1 - \tilde{\mathsf{P}}_{\text{dt}})^{\eta - |B_{\text{dt}}|}} \quad (103)\end{aligned}$$

3) Analyzing $\mathbb{P}[\mathcal{E}_{\mathsf{e},2} | \mathcal{B}_{detect} = B_{dt}]$: To evaluate this probability, we first follow the argument provided in Appendix A, and introduce a new metric:

$$\begin{aligned}&\tilde{i}_{\text{TIN}}^{(\mathsf{e})}(\mathbf{s}_{\mathsf{e},2}, \mathbf{s}_{\mathsf{e},1}; \mathbf{y}_c | \mathcal{B}_{\text{detect}} = B_{\text{dt}}) \\ &= \sum_{b \notin B_{\text{dt}}} \sum_{j=1}^{q} \log \frac{Q_{\boldsymbol{Y}_{b,c,j} | \boldsymbol{S}_{b,j}^{(1)}}(\boldsymbol{y}_{b,c,j} | \boldsymbol{s}_{b,j}^{(1)})}{Q_{\boldsymbol{Y}_{b,c,j}}(\boldsymbol{y}_{b,c,j})} \\ &\quad + \sum_{b \in B_{\text{dt}}} \sum_{j=1}^{q} \log \frac{Q_{\boldsymbol{Y}_{b,c,j} | \boldsymbol{S}_{b,j}^{(2)}}(\boldsymbol{y}_{b,c,j} | \boldsymbol{s}_{b,j}^{(2)})}{Q_{\boldsymbol{Y}_{b,c,j}}(\boldsymbol{y}_{b,c,j})}, \quad (104)\end{aligned}$$

where Qs are Gaussian distributions. Specifically, $Q_{\boldsymbol{Y}_{b,c,j}}(\boldsymbol{y}_{b,c,j})$ is defined in (87) and

$$Q_{\boldsymbol{Y}_{b,c,j} | \boldsymbol{S}_{b,j}^{(1)}} \sim \mathcal{N}\left(\boldsymbol{y}_{b,c,j} : \lambda_{b,j} \boldsymbol{s}_{b,j}^{(1)}, \sigma^2_{y|s^{(1)},j} \mathbf{I}_{\ell \times \ell}\right), \quad (105)$$

$$Q_{\boldsymbol{Y}_{b,c,j} | \boldsymbol{S}_{b,j}^{(2)}} \sim \mathcal{N}\left(\boldsymbol{y}_{b,c,j} : \lambda_{b,j}(1 - \alpha_u)^2 \boldsymbol{s}_{b,j}^{(2)}, \sigma^2_{y|s^{(2)},j} \mathbf{I}_{\ell \times \ell}\right), \quad (106)$$

where $\sigma^2_{y|s^{(1)},j}$ and $\sigma^2_{y|s^{(2)},j}$ are defined in (56) and (57), respectively. Following the same argument as the proof of Lemma 5 in [**?**, Appendix E], we have the following lemma showing $\tilde{i}_{\text{TIN}}^{(\mathsf{e})}(\mathbf{s}_{\mathsf{e},2}, \mathbf{s}_{\mathsf{e},1}; \mathbf{y}_c | \mathcal{B}_{\text{detect}} = B_{\text{dt}})$ converges in distribution to a Gaussian distribution.

Lemma 6: The following holds:

$$\tilde{i}_{\text{TIN}}^{(\mathsf{e})}(\mathbf{s}_{\mathsf{e},2}, \mathbf{s}_{\mathsf{e},1}; \mathbf{y}_c | \mathcal{B}_{\text{detect}} = B_{\text{dt}}) \sim \mathcal{N}(n\tilde{\mathsf{C}}_{\mathsf{e}}, n\tilde{\mathsf{V}}_{\mathsf{e}}), \quad (107)$$

where $\tilde{\mathsf{C}}_{\mathsf{e}}$ and $\tilde{\mathsf{V}}_{\mathsf{e}}$ are defined in (51) and (52), respectively.
Now by using the threshold bound for maximum-metric decoding, for any given threshold δ_{e}, we have

$$\begin{aligned}&\mathbb{P}[\mathcal{E}_{\mathsf{e},2} | \mathcal{B}_{\text{detect}} = B_{\text{dt}}] \\ &\leq \mathbb{P}[\tilde{i}_{\text{TIN}}^{(\mathsf{e})}(\mathbf{S}_{\mathsf{e},1}, \mathbf{S}_{\mathsf{e},2}; \mathbf{Y}_c | \mathcal{B}_{\text{detect}} = B_{\text{dt}}) \leq \delta_{\mathsf{e}}] \\ &+ (M_{\mathsf{e}} M_{\mathsf{s}} - 1)\mathbb{P}[\tilde{i}_{\text{TIN}}^{(\mathsf{e})}(\bar{\mathbf{S}}_{\mathsf{e},1}, \bar{\mathbf{S}}_{\mathsf{e},2}; \mathbf{Y}_c | \mathcal{B}_{\text{detect}} = B_{\text{dt}}) > \delta_{\mathsf{e}}], \quad (108)\end{aligned}$$

where $\bar{\mathbf{S}}_{\mathsf{e},1} \sim f_{\mathbf{S}_{\mathsf{e},1}}$ and $\bar{\mathbf{S}}_{\mathsf{e},2} \sim f_{\mathbf{S}_{\mathsf{e},2}}$ and are independent of $\mathbf{S}_{\mathsf{e},1}$, $\mathbf{S}_{\mathsf{e},2}$ and $\mathbf{Y}_c$. For some $K_{\mathsf{e}} > 0$, set

$$\delta_{\mathsf{e}} := \log M_{\mathsf{e}} + \log M_{\mathsf{s}} + K_{\mathsf{e}} \log(n). \quad (109)$$

To evaluate $\mathbb{P}[\tilde{i}_{\text{TIN}}^{(\mathsf{e})}(\mathbf{S}_{\mathsf{e},1}, \mathbf{S}_{\mathsf{e},2}; \mathbf{Y}_c | \mathcal{B}_{\text{detect}} = B_{\text{dt}}) \leq \delta_{\mathsf{e}}]$, given that $\tilde{i}_{\text{TIN}}^{(\mathsf{e})}(\mathbf{S}_{\mathsf{e},1}, \mathbf{S}_{\mathsf{e},2}; \mathbf{Y}_c | \mathcal{B}_{\text{detect}} = B_{\text{dt}})$ follows a Gaussian distribution (see Lemma 6), we employ the Berry-Esseen CLT for functions to bound this probability. Hence,

$$\begin{aligned}&\mathbb{P}[\tilde{i}_{\text{TIN}}^{(\mathsf{e})}(\mathbf{S}_{\mathsf{e},1}, \mathbf{S}_{\mathsf{e},2}; \mathbf{Y}_c | \mathcal{B}_{\text{detect}} = B_{\text{dt}}) \leq \delta_{\mathsf{e}}] \\ &\leq Q\left(\frac{-\log(M_{\mathsf{e}}) - \log(M_{\mathsf{s}}) + n\tilde{\mathsf{C}}_{\mathsf{e}} - K_{\mathsf{e}} \log(n)}{\sqrt{n\tilde{\mathsf{V}}_{\mathsf{e}}}}\right) + \frac{\tilde{B}}{\sqrt{n}}, \quad (110)\end{aligned}$$

for some $\tilde{B} > 0$ and where $Q(\cdot)$ is the Q-function. To evaluate $\mathbb{P}[\tilde{i}_{\text{TIN}}^{(\mathsf{e})}(\bar{\mathbf{S}}_{\mathsf{e},1}, \bar{\mathbf{S}}_{\mathsf{e},2}; \mathbf{Y}_c | \mathcal{B}_{\text{detect}} = B_{\text{dt}}) > \delta_{\mathsf{e}}]$ we follow [35, Lemma 47] which results in

$$\begin{aligned}&\mathbb{P}[\tilde{i}_{\text{TIN}}^{(\mathsf{e})}(\bar{\mathbf{S}}_{\mathsf{e},1}, \bar{\mathbf{S}}_{\mathsf{e},2}; \mathbf{Y}_c | \mathcal{B}_{\text{detect}} = B_{\text{dt}}) > \delta_{\mathsf{e}}] \\ &\leq \frac{2}{M_{\mathsf{e}} M_{\mathsf{s}} n^{K_{\mathsf{e}}}} \left(\frac{\log 2}{\sqrt{2\pi n}} + \frac{2\tilde{B}}{\sqrt{n}}\right). \quad (111)\end{aligned}$$

By combining (60), (100), (103), (108), (110) and (111) we have the following bound:

$$\begin{aligned}\epsilon_{\mathsf{e}}^{(n)} &\overset{(i)}{\leq} 1 + \frac{\tilde{B}}{\sqrt{n}}\left(1 + \frac{4}{n^{K_{\mathsf{e}}}}\right) + \frac{2\log 2}{n^{K_{\mathsf{e}}}\sqrt{2n\pi}} \\ &\quad - \sum_{B_{\text{dt}}} \left(P_{b-1,\mathsf{D}}(1 - (\tilde{\epsilon}_{\text{U},1})^{M_{\text{U}} M_v})\right)^{|B_{\text{dt}}|} \\ &\qquad \times ((1 - P_{b-1,\mathsf{D}})(1 - P_{\text{U},2}))^{\eta - |B_{\text{dt}}|} \\ &\quad + \sum_{B_{\text{dt}}} \mathsf{P}_{\text{dt}}^{|B_{\text{dt}}|}(1 - \mathsf{P}_{\text{dt}})^{\eta - |B_{\text{dt}}|} \\ &\qquad Q\left(\frac{-\log(M_{\mathsf{e}} M_{\mathsf{s}}) + n\tilde{\mathsf{C}}_{\mathsf{e}} - K_{\mathsf{e}} \log(n)}{\sqrt{n\tilde{\mathsf{V}}_{\mathsf{e}}}}\right) \quad (112) \\ &= \Delta_{\mathsf{e}} + \sum_{B_{\text{dt}}} \mathsf{P}_{\text{dt}}^{|B_{\text{dt}}|}(1 - \mathsf{P}_{\text{dt}})^{\eta - |B_{\text{dt}}|} \\ &\qquad Q\left(\frac{-\log(M_{\mathsf{e}} M_{\mathsf{s}}) + n\tilde{\mathsf{C}}_{\mathsf{e}} - K_{\mathsf{e}} \log(n)}{\sqrt{n\tilde{\mathsf{V}}_{\mathsf{e}}}}\right), \quad (113)\end{aligned}$$

where Δ_{e} is defined in (54) and (i) is followed by (91) and (93) which also result in $\tilde{\mathsf{P}}_{\text{dt}} \leq \mathsf{P}_{\text{dt}}$ where P_{dt} is defined in (53). According to Proposition 1, it is required that $\epsilon_{\mathsf{e}}^{(n)}$ to be bounded above by ϵ_{e}, i.e., $\epsilon_{\mathsf{e}}^{(n)} \leq \epsilon_{\mathsf{e}}$. Thus

$$\begin{aligned}\epsilon_{\mathsf{e}} &\geq \Delta_{\mathsf{e}} + \sum_{B_{\text{dt}}} \mathsf{P}_{\text{dt}}^{|B_{\text{dt}}|}(1 - \mathsf{P}_{\text{dt}})^{\eta - |B_{\text{dt}}|} \\ &\qquad Q\left(\frac{-\log(M_{\mathsf{e}} M_{\mathsf{s}}) + n\tilde{\mathsf{C}}_{\mathsf{e}} - K_{\mathsf{e}} \log(n)}{\sqrt{n\tilde{\mathsf{V}}_{\mathsf{e}}}}\right) \quad (114) \\ &\overset{(i)}{\geq} \Delta_{\mathsf{e}} + Q\left(\frac{-\log(M_{\mathsf{e}} M_{\mathsf{s}}) + n\mathsf{C}_{\mathsf{e}} - K_{\mathsf{e}} \log(n)}{\sqrt{n\mathsf{V}_{\mathsf{e}}}}\right) \quad (115)\end{aligned}$$

where C_{e} and V_{e} are defined in (49) and (50), respectively, and (i) follows by the fact that Q-function is a decreasing function of its argument. By taking the inverse of the Q-function and dividing both sides by n, we conclude the proof.

APPENDIX C
PROOF OF LEMMA 3

Recall the average decoding eMBB error probability under the SIC approach from (60). In this section, we analyze $\mathbb{P}[\mathcal{B}_{\text{decode}} = B_{\text{dc}}|\mathcal{B}_{\text{detect}} = \mathcal{B}_{\text{URLLC}}, \mathcal{B}_{\text{detect}} = B_{\text{dt}}]$ and $\mathbb{P}[\mathcal{E}_{\mathsf{e},2}|\mathcal{B}_{\text{detect}} = B_{\text{dt}}, \mathcal{B}_{\text{decode}} = B_{\text{dc}}]$. See Appendix B for the calculation of the remaining terms in the RHS of (60).

A. Analyzing $\mathbb{P}[\mathcal{B}_{decode} = B_{dc}|\mathcal{B}_{detect} = \mathcal{B}_{URLLC}, \mathcal{B}_{detect} = B_{dt}]$

From (92), we have

$$\mathbb{P}[m_{b,\mathsf{U}} \neq \hat{m}_{b,\mathsf{U}}|\mathcal{B}_{\text{detect}} = \mathcal{B}_{\text{URLLC}} = B_{\text{dt}}] \leq \tilde{\epsilon}_{\mathsf{U},1} + \tilde{\epsilon}_{\mathsf{U},2}. \quad (116)$$

Let $\tilde{\epsilon}_{\mathsf{U},1} + \tilde{\epsilon}_{\mathsf{U},2} := 1 - \mathsf{P}_{\text{dc}}$. Thus,

$$\begin{aligned}
&\mathbb{P}[\mathcal{B}_{\text{decode}} = B_{\text{dc}}|\mathcal{B}_{\text{detect}} = \mathcal{B}_{\text{URLLC}}, \mathcal{B}_{\text{detect}} = B_{\text{dt}}] \\
&= \prod_{b\in B_{\text{dc}}} \mathbb{P}[m_{b,\mathsf{U}} = \hat{m}_{b,\mathsf{U}}|\mathcal{B}_{\text{detect}} = \mathcal{B}_{\text{URLLC}} = B_{\text{dt}}] \\
&\quad \cdot \prod_{b\in B_{\text{dt}}\setminus B_{\text{dc}}} (1 - \mathbb{P}[m_{b,\mathsf{U}} = \hat{m}_{b,\mathsf{U}}|\mathcal{B}_{\text{detect}} = \mathcal{B}_{\text{URLLC}} = B_{\text{dt}}]) \quad (117) \\
&\leq \mathsf{P}_{\text{dc}}^{|B_{\text{dc}}|}(1 - \mathsf{P}_{\text{dc}})^{|B_{\text{dt}}|-|B_{\text{dc}}|}. \quad (118)
\end{aligned}$$

which is equivalent to the probability that all the URLLC messages in B_{dc} are decoded correctly and no URLLC message is decoded correctly in the remaining blocks in $B_{\text{dt}}\setminus B_{\text{dc}}$.

B. Analyzing $\mathbb{P}[\mathcal{E}_{\mathsf{e},2}|\mathcal{B}_{detect} = B_{dt}, \mathcal{B}_{decode} = B_{dc}]$

To evaluate this probability, we first follow the argument provided in Appendix A, and introduce a new metric:

$$\begin{aligned}
&\tilde{i}^{(\mathsf{e})}_{\text{SIC}}(\mathbf{s}_{\mathsf{e},2}, \mathbf{s}_{\mathsf{e},1}; \mathbf{y}_c|\mathcal{B}_{\text{detect}} = B_{\text{dt}}, \mathcal{B}_{\text{decode}} = B_{\text{dc}}) := \\
&\log \prod_{b\notin B_{\text{dt}}} \frac{Q_{\mathbf{Y}_{b,c}|\mathbf{S}_b^{(1)}}(\mathbf{y}_{b,c}|\mathbf{s}_b^{(1)})}{Q_{\mathbf{Y}_{b,c}}(\mathbf{y}_{b,c})} + \log \prod_{b\in B_{\text{dt}}\setminus B_{\text{dc}}} \frac{Q_{\mathbf{Y}_{b,c}|\mathbf{S}_b^{(2)}}(\mathbf{y}_{b,c}|\mathbf{s}_b^{(2)})}{Q_{\mathbf{Y}_{b,c}}(\mathbf{y}_{b,c})} \\
&+ \log \prod_{b\in B_{\text{dc}}} \frac{Q_{\mathbf{Y}_{b,c}|\mathbf{S}_b^{(2)},\mathbf{V}_b}(\mathbf{y}_{b,c}|\mathbf{s}_b^{(2)}, \mathbf{v}_b)}{Q_{\mathbf{Y}_{b,c}|\mathbf{V}_b}(\mathbf{y}_{b,c}|\mathbf{v}_b)}, \quad (119)
\end{aligned}$$

where Qs are Gaussian distributions. Specifically, $Q_{\boldsymbol{Y}_{b,c,j}}(\boldsymbol{y}_{b,c,j})$, $Q_{\mathbf{Y}_{b,c}|\mathbf{V}_b}(\mathbf{y}_{b,c}|\mathbf{v}_b)$, $Q_{\mathbf{Y}_{b,c}|\mathbf{S}_b^{(1)}}(\mathbf{y}_{b,c}|\mathbf{s}_b^{(1)})$, and $Q_{\mathbf{Y}_{b,c}|\mathbf{S}_b^{(2)}}(\mathbf{y}_{b,c}|\mathbf{s}_b^{(2)})$ are defined in (87), (88), (105) and (106), respectively, and $Q_{\mathbf{Y}_{b,c}|\mathbf{S}_b^{(2)},\mathbf{V}_b}(\mathbf{y}_{b,c}|\mathbf{s}_b^{(2)}, \mathbf{v}_b)$ is a Gaussian distribution with mean $\boldsymbol{V}_{b,j} + (1-\alpha_u)\boldsymbol{S}_{b,j}^{(1)}$ and variance $\sigma^2_{y|s^{(2)}v,j}$ defined in (69). Following the same argument as the proof of Lemma 5, we have the following lemma.

Lemma 7: The following holds:

$$\tilde{i}^{(\mathsf{e})}_{\text{SIC}}(\mathbf{s}_{\mathsf{e},2}, \mathbf{s}_{\mathsf{e},1}; \mathbf{y}_c|\mathcal{B}_{\text{detect}} = B_{\text{dt}}, \mathcal{B}_{\text{decode}} = B_{\text{dc}}) \sim \mathcal{N}(n\tilde{\mathsf{C}}_{\mathsf{e},2}, n\tilde{\mathsf{V}}_{\mathsf{e},2}), \quad (120)$$

where $\tilde{\mathsf{C}}_{\mathsf{e},2}$ and $\tilde{\mathsf{V}}_{\mathsf{e},2}$ are defined in (64) and (65), respectively.

Following similar steps as in (108) to (113), we can show that

$$\begin{aligned}
\epsilon_{\mathsf{e}} &\geq \Delta_{\mathsf{e}} \\
&+ \sum_{B_{\text{dt}}} \mathsf{P}_{\text{dt}}^{|B_{\text{dt}}|}(1-\mathsf{P}_{\text{dt}})^{\eta-|B_{\text{dt}}|} \sum_{B_{\text{dc}}} \mathsf{P}_{\text{dc}}^{|B_{\text{dc}}|}(1-\mathsf{P}_{\text{dc}})^{|B_{\text{dt}}|-|B_{\text{dc}}|} \\
&\qquad Q\left(\frac{-\log(M_{\mathsf{e}}M_{\mathsf{s}}) + n\tilde{\mathsf{C}}_{\mathsf{e},2} - K_{\mathsf{e}}\log(n)}{\sqrt{n\tilde{\mathsf{V}}_{\mathsf{e},2}}}\right) \quad (121) \\
&\geq \Delta_{\mathsf{e}} + Q\left(\frac{-\log(M_{\mathsf{e}}M_{\mathsf{s}}) + n\mathsf{C}_{\mathsf{e},2} - K_{\mathsf{e},2}\log(n)}{\sqrt{n\mathsf{V}_{\mathsf{e},2}}}\right) \quad (122)
\end{aligned}$$

where $\mathsf{C}_{\mathsf{e},2}$ and $\mathsf{V}_{\mathsf{e},2}$ are defined in (62) and (63), respectively. By taking the inverse of the Q-function and dividing both sides by n, we conclude the proof.

APPENDIX D
PROOF OF LEMMA 4

From (78), the probability of false alarm is given by

$$\begin{aligned}
P_{b,\text{FA}} &= \mathbb{P}\left[\sum_{j=1}^{q}\left(||\boldsymbol{N}_{b,s,j}||^2 - \frac{||\boldsymbol{N}_{b,s,j} - \boldsymbol{\mu}_{b,j}||^2}{\sigma^2_{b,j}}\right) > \delta\right] \quad (123) \\
&= \mathbb{P}\left[u_b > \delta + \sum_{j=1}^{q}\frac{1}{\sigma^2_{b,j}-1}||\boldsymbol{\mu}_{b,j}||^2\right], \quad (124)
\end{aligned}$$

where

$$u_b := \sum_{j=1}^{q}\left(1 - \frac{1}{\sigma^2_{b,j}}\right)||\boldsymbol{N}_{b,s,j} + \frac{1}{\sigma^2_{b,j}-1}\boldsymbol{\mu}_{b,j}||^2. \quad (125)$$

Given that $\boldsymbol{N}_{b,s,j} \sim \mathcal{N}(\mathbf{0}, \mathbf{I}_\ell)$, then $\boldsymbol{N}_{b,s,j} + \frac{1}{\sigma^2_{b,j}-1}\boldsymbol{\mu}_{b,j} \sim \mathcal{N}(\frac{1}{\sigma^2_{b,j}-1}\boldsymbol{\mu}_{b,j}, \mathbf{I}_\ell)$ and consequently $||\boldsymbol{N}_{b,s,j} + \frac{1}{\sigma^2_{b,j}-1}\boldsymbol{\mu}_{b,j}||^2$ follows a non-central chi-square distribution with degree of ℓ and parameter $\frac{1}{(\sigma^2_{b,j}-1)^2}||\boldsymbol{\mu}_{b,j}||^2$. Hence, u_b is the weighted sum of independent non-central chi-square random variables. It thus follows a generalized chi-square distribution. More specifically,

$$u_b \sim \tilde{\mathcal{X}}_1(\{w_{b,j}\}_{j=1}^q, \ell, \{\nu_{b,j}\}_{j=1}^q), \quad (126)$$

where the parameters $\{w_{b,j}\}_{j=1}^q$ and $\{\nu_{b,j}\}_{j=1}^q$ are defined in (81). Let $F_{\tilde{\mathcal{X}}_1}(\cdot)$ denote the CDF of the corresponding generalized chi-square distribution. The probability of false alarm thus is given by

$$P_{b,\text{FA}} = 1 - F_{\tilde{\mathcal{X}}_1}\left(\delta + \sum_{j=1}^{q}\frac{1}{\sigma^2_{b,j}-1}||\boldsymbol{\mu}_{b,j}||^2\right). \quad (127)$$

For each block b, we fix $P_{b,\text{FA}}$ at P_{FA}. Thus, δ is equal to

$$\delta = F^{-1}_{\tilde{\mathcal{X}}_1}(1 - P_{\text{FA}}) - \sum_{j=1}^{q}\frac{1}{\sigma^2_{b,j}-1}||\boldsymbol{\mu}_{b,j}||^2. \quad (128)$$

The target detection probability is given by

$$P_{b,\mathsf{D}} = \mathbb{P}\Big[\sum_{j=1}^{q}\Big(||\boldsymbol{N}_{b,s,j} + \boldsymbol{X}_{b,j}\sqrt{\gamma_{b,j}}||^2$$

$$-\frac{||\boldsymbol{N}_{b,s,j}+\boldsymbol{X}_{b,j}\sqrt{\gamma_{b,j}}-\boldsymbol{\mu}_{b,j}||^2}{\sigma^2_{b,j}}\Big)>\delta\Big] \quad (129)$$

$$=\mathbb{P}[\tilde{u}_b>F^{-1}_{\tilde{\mathcal{X}}_1}(1-P_{\text{FA}})], \quad (130)$$

where

$$\tilde{u}_b:=\sum_{j=1}^{q}(1-\frac{1}{\sigma^2_{b,j}})||\boldsymbol{N}_{b,s,j}+\sqrt{\gamma_{b,j}}\boldsymbol{X}_{b,j}+\frac{1}{\sigma^2_{b,j}-1}\boldsymbol{\mu}_{b,j}||^2. \quad (131)$$

Following the same argument provided for the false alarm probability, one can obtain that $\tilde{u}_b$ is the weighted sum of independent non-central chi-square random variables and thus follows a generalized chi-square distribution as

$$\tilde{u}_b\sim\tilde{\mathcal{X}}_2(\{w_{b,j}\}_{j=1}^q,\ell,\{\tilde{\nu}_{b,j}\}_{j=1}^q), \quad (132)$$

where the parameters $\{w_{b,j}\}_{j=1}^q$ and $\{\tilde{\nu}_{b,j}\}_{j=1}^q$ are defined in (81). By denoting $F_{\tilde{\mathcal{X}}_2}(\cdot)$ as the CDF of the corresponding generalized chi-square distribution, we conclude the proof.

Appendix E
Proof of Lemma 5

To prove this lemma, we follow a similar argument as the one provided in [33, Proposition 1]. Recall the definition of $\tilde{i}_{\mathsf{U}}(\mathbf{V}_b;\mathbf{Y}_{b,c})$ from (86). In the following, we prove that

$$\tilde{i}_{\mathsf{U}}(\boldsymbol{V}_{b,j};\boldsymbol{Y}_{b,c,j})\sim\mathcal{N}\left(\ell\mathsf{C}(\Omega_{b,j}),\ell\mathsf{V}(\Omega_{b,j})\right) \quad (133)$$

which consequently proves Lemma 5. To this end, recall the definition of $Q_{\boldsymbol{Y}_{b,c,j}|\boldsymbol{V}_{b,j}}(\boldsymbol{y}_{b,c,j}|\boldsymbol{v}_{b,j})$ and $Q_{\boldsymbol{Y}_{b,c,j}}(\boldsymbol{y}_{b,c,j})$ from (87) and (88), respectively. Denote

$$\tilde{\boldsymbol{Z}}_j=\lambda_{b,j}(1-\alpha_u)(\boldsymbol{S}^{(2)}_{b,j}+(1-\alpha_{s,2})\boldsymbol{X}^{(\mathsf{s},2)}_{b,j})+\boldsymbol{N}_{b,c,j}. \quad (134)$$

According to the definition of $Q_{\boldsymbol{Y}_{b,c,j}|\boldsymbol{V}_{b,j}}(\boldsymbol{y}_{b,c,j}|\boldsymbol{v}_{b,j})$, $\tilde{\boldsymbol{Z}}_j$ follows an i.i.d Gaussian distribution with zero mean and variance $\sigma^2_{y|v,j}\mathbf{I}_{\ell\times\ell}$. We thus have

$$\tilde{i}_{\mathsf{U}}(\boldsymbol{V}_{b,j};\boldsymbol{Y}_{b,c,j})=\log\frac{Q_{\boldsymbol{Y}_{b,c,j}|\boldsymbol{V}_{b,j}}(\boldsymbol{y}_{b,c,j}|\boldsymbol{v}_{b,j})}{Q_{\boldsymbol{Y}_{b,c,j}}(\boldsymbol{y}_{b,c,j})} \quad (135)$$

$$=\log\frac{\left(\frac{1}{\sqrt{2\pi\sigma^2_{y|v,j}}}\right)^{\ell}\exp\left[-\frac{||\boldsymbol{Y}_{b,c,j}-\sqrt{\lambda_{b,j}}\boldsymbol{V}_{b,j}||^2}{2\sigma^2_{y|v,j}}\right]}{\left(\frac{1}{\sqrt{2\pi\sigma^2_{y,j}}}\right)^{\ell}\exp\left[-\frac{||\boldsymbol{Y}_{b,c,j}||^2}{2\sigma^2_{y,j}}\right]} \quad (136)$$

$$=\ell\mathsf{C}(\Omega_{b,j})+\frac{1}{2\sigma^2_{y,j}}\Big(||\boldsymbol{Y}_{b,c,j}||^2-\frac{\sigma^2_{y,j}}{\sigma^2_{y|v,j}}||\tilde{\boldsymbol{Z}}_j||^2\Big) \quad (137)$$

$$=\ell\mathsf{C}(\Omega_{b,j})+\frac{1}{2\sigma^2_{y,j}}\left(\sigma^2_{y,j}-\sigma^2_{y|v,j}\right)\left(\ell-\frac{||\tilde{\boldsymbol{Z}}_j||^2}{\sigma^2_{y|v,j}}\right)+\frac{\sqrt{\lambda_{b,j}}}{\sigma^2_{y,j}}\langle\boldsymbol{V}_{b,j},\tilde{\boldsymbol{Z}}_j\rangle \quad (138)$$

$$=\ell\mathsf{C}(\Omega_{b,j})+\frac{1}{2\sigma^2_{y,j}}\Big(c_1(\ell-||\tilde{\boldsymbol{Z}}_j||^2)+c_2\langle\tilde{\boldsymbol{Z}}_j,\boldsymbol{V}_{b,j}\rangle\Big) \quad (139)$$

where

$$c_1:=\Omega_{b,j}\sigma^2_{y|v,j}, \quad (140)$$

$$c_2:=2\sqrt{\lambda_{b,j}}. \quad (141)$$

The summands in (139) are not independent, since $\boldsymbol{V}_{b,j}$ are not independent across time. One can however express independent uniform random variables on the power shell as a functions of independent Gaussian random variables. To this end, let $\boldsymbol{W}_1\sim\mathcal{N}(0,I_\ell)$ be i.i.d Gaussian random variables independent of the noise $\tilde{\boldsymbol{Z}}_j$. Inputs $V_{b,j,t}$ with $t\in[\ell]$ thus can be expressed as

$$V_{b,j,t}=\sqrt{\ell(\beta_u+\alpha_u^2(1-\beta_u))\mathsf{P}}\frac{W_{1,t}}{||\boldsymbol{W}_1||}. \quad (142)$$

To apply the CLT for functions proposed in [33, Proposition 1], we consider the sequence $\{\boldsymbol{U}_t:=(U_{1,t},U_{2,t},U_{3,t})\}_{t=1}^{\infty}$ whose elements are defined as

$$U_{1,t}:=1-\frac{\tilde{Z}^2_{j,t}}{\sigma^2_{y|v,j}}, \quad (143)$$

$$U_{2,t}:=\sqrt{(\beta_u+\alpha_u^2(1-\beta_u))\mathsf{P}\sigma^2_{y|v,j}}W_{1,t}\tilde{Z}_{j,t}, \quad (144)$$

$$U_{3,t}:=W^2_{1,t}-1, \quad (145)$$

Note that this random vector has an i.i.d. distribution across time $t=1,\dots,n$ and its moments can be easily verified to satisfy $\mathbb{E}[\boldsymbol{U}_1]=0$ and $\mathbb{E}[||\boldsymbol{U}_t||_2^3]<\infty$. The covariance matrix of this vector is given by

$$\text{Cov}(\boldsymbol{U})=\text{Diag}\left[2,(\beta_u+\alpha_u^2(1-\beta_u))\mathsf{P}\sigma^2_{y|v,j},2\right]. \quad (146)$$

Next, we define the function f as

$$f(\boldsymbol{u})=c_1u_1+\frac{c_2u_2}{\sqrt{1+u_3}}. \quad (147)$$

Notice that $f(\mathbf{0})=0$, and all the first and second order partial derivatives of f are continuous in a neighborhood of $\boldsymbol{u}=0$. The Jacobian matrix $\{\frac{\partial f(\boldsymbol{u})}{\partial u_j}\}_{1\times3}$ at $\boldsymbol{u}=0$ thus is given by

$$\mathrm{J}\Big|_{\boldsymbol{u}=0}=[c_1\ c_2\ 0]. \quad (148)$$

Furthermore,

$$f\left(\frac{1}{\ell}\sum_{t=1}^{\ell}\boldsymbol{U}_t\right)=\frac{c_1}{\ell}\sum_{t=1}^{\ell}\left(1-\frac{\tilde{Z}^2_{j,t}}{\sigma^2_{y|v,j}}\right)+\frac{\frac{c_2}{\ell}\sum_{t=1}^{\ell}\frac{\sqrt{(\beta_u+\alpha_u^2(1-\beta_u))\mathsf{P}\sigma^2_{y|v,j}}}{\sqrt{\ell}}W_{1,t}\tilde{Z}_{j,t}}{\sqrt{1+\frac{1}{\ell}\sum_{t=1}^{\ell}(W^2_{1,t}-1)}}$$

$$=\frac{1}{\ell}\Big(c_1(\ell-||\tilde{\boldsymbol{Z}}_j||^2)+c_2\langle\tilde{\boldsymbol{Z}}_j,\boldsymbol{V}_{b,j}\rangle\Big) \quad (149)$$

From the CLT in [33, Proposition 1], we now conclude that the random variable $\tilde{i}_{\mathsf{U}}(\boldsymbol{V}_{b,j};\boldsymbol{Y}_{b,c,j})$ converges in distribution to a Gaussian distribution with mean $\ell\mathsf{C}(\Omega_{b,j})$ and variance

$$\frac{\ell}{4\sigma^4_{y,j}}[c_1\ c_2\ 0\ 0]\text{Cov}(\boldsymbol{U})[c_1\ c_2\ 0]^T=\frac{\ell}{4\sigma^4_{y,j}}\left[2\Omega^2_{b,j}\sigma^4_{y|v,j}+4\lambda_{b,j}(\beta_u+\alpha_u^2(1-\beta_u))\mathsf{P}\sigma^2_{y|v,j}\right]$$

$$= \ell \frac{\Omega_{b,j}(2+\Omega_{b,j})}{2(1+\Omega_{b,j})^2} = \mathsf{V}(\Omega_{b,j}) \tag{150}$$

This concludes the proof.

REFERENCES

[1] H. Nikbakht, Y. C. Eldar, and H. V. Poor, "A MIMO ISAC system for ultra-reliable and low-latency communications," arXiv:2501.13025, 2025.

[2] V. Koivunen, M. F. Keskin, H. Wymeersch, M. Valkama, and N. González-Prelcic, "Multicarrier ISAC: Advances in waveform design, signal processing, and learning under nonidealities," *IEEE Signal Processing Magazine*, vol. 41, no. 5, pp. 17–30, Sept. 2024.

[3] H. Li, Z. Han and H. V. Poor, "Waveform shaping in integrated sensing and communications," in *Proceedings of the IEEE Military Communications Conference*, Washington, DC, USA, pp. 670–671, 2024.

[4] Y. Liu, T. Huang, F. Liu, D. Ma, W. Huangfu, and Y. C. Eldar, "Next-generation multiple access for integrated sensing and communications," *Proceedings of the IEEE*, vol. 112, no. 9, pp. 1467–1496, Sept. 2024.

[5] F. Liu et al., "Integrated sensing and communications: Toward dual-functional wireless networks for 6G and beyond," *IEEE Journal on Selected Areas in Communications*, vol. 40, no. 6, pp. 1728–1767, June 2022.

[6] M. Hatami, N. Nguyen, and M. Juntti, "Waveform design for multi-carrier multiuser MIMO joint communications and sensing," in *Proceedings of the IEEE International Workshop on Signal Processing Advances in Wireless Communications*, Lucca, Italy, pp. 346–350, 2024.

[7] M. Mittelbach, R. F. Schaefer, M. Bloch, A. Yener, and O. Günlü, "Sensing-assisted secure communications over correlated Rayleigh fading channels," *Entropy*, vol. 27, no. 3, p. 225, Mar. 2025.

[8] H. Wu and H. Joudeh, "On joint communication and channel discrimination," in *Proceedings of the IEEE International Symposium on Information Theory*, Espoo, Finland, pp. 3321–3326, Jun. 2022.

[9] Y. Niu, Z. Wei, L. Wang, H. Wu, and Z. Feng, "Interference management for integrated sensing and communication systems: A survey," *IEEE Internet of Things Journal*, vol. 12, no. 7, pp. 8110–8134, April, 2025.

[10] N. H. Mahmood, I. Atzeni, E. A. Jorswieck, and O. L. A. López, "Ultra-reliable low-latency communications: Foundations, enablers, system design, and evolution towards 6G," *Foundations and Trends® in Communications and Info. Theory*, vol. 20, no. 5-6, pp. 512–747, 2023.

[11] P. Qin, Y. Fu, Z. Yu, J. Zhang, and X. Zhao, "URLLC-aware trajectory plan and beamforming design for NOMA-aided UAV integrated sensing, communication, and computation networks," *IEEE Transactions on Vehicular Technology*, vol. 74, no. 1, pp. 1610–1625, Jan. 2025.

[12] L. B. Luat, N. C. Luong and D. I. Kim, "Integrated radar and communication in ultra-reliable and low-latency communications-enabled UAV networks," *IEEE Transactions on Vehicular Technology*, 2025.

[13] A. Pourkabirian, M. S. Kordafshari, A. Jindal and M. H. Anisi, "A vision of 6G URLLC: Physical-layer technologies and enablers," *IEEE Communications Standards Magazine*, vol. 8, no. 2, pp. 20–27, June 2024.

[14] S. Kurma et al., "URLLC-enabled full-duplex cell-free massive MIMO systems with mobility," *IEEE Open Journal of the Communications Society*, vol. 5, pp. 3196–3211, 2024.

[15] J. Singh, B. Naveen, S. Srivastava, A. K. Jagannatham, and L. Hanzo, "Pareto optimal hybrid beamforming for short-packet millimeter-wave integrated sensing and communication," *IEEE Transactions on Communications*, Dec. 2024.

[16] C. Ding, C. Zeng, C. Chang, J.-B. Wang, and M. Lin, "Joint precoding for MIMO radar and URLLC in ISAC systems," in *Proceedings of the 1st ACM MobiCom Workshop on Integrated Sensing and Communications Systems*, pp. 12–18, 2022.

[17] Z. Behdad, Ö. T. Demir, K. W. Sung, and C. Cavdar, "Interplay Between Sensing and Communication in Cell-Free Massive MIMO with URLLC Users," in *Proceedings of the IEEE Wireless Communications and Networking Conference*, Dubai, United Arab Emirates, pp. 1-6, 2024.

[18] X. Zhao and Y. J. Angela Zhang, "Joint beamforming and scheduling for integrated sensing and communication systems in URLLC: A POMDP approach," *IEEE Transactions on Communications*, vol. 72, no. 10, pp. 6145–6161, Oct. 2024.

[19] N. Keshtiarast, P. K. Bishoyi, and Marina Petrova, "Environment-aware scheduling of URLLC and sensing services for smart industries," arXiv:2503.05313, 2025.

[20] H. Nikbakht, M. Wigger, M. Egan, S. Shamai (Shitz), J-M. Gorce, and H. V. Poor, "An information-theoretic view of mixed-delay traffic in 5G and 6G," *Entropy*, vol. 24, no. 5, article 637, 2022.

[21] X. Song and M. Yuan, "Performance analysis of one-way highway vehicular networks with dynamic multiplexing of eMBB and URLLC traffics," *IEEE Access*, vol. 7, pp. 118020–118029, 2019.

[22] G. Interdonato, S. Buzzi, C. D'Andrea, L. Venturino, C. D'Elia, and P. Vendittelli, "On the coexistence of eMBB and URLLC in multi-cell massive MIMO," *IEEE Open Journal of the Communications Society*, vol. 4, pp. 1040–1059, 2023.

[23] H. Nikbakht, E. Ruzomberka, M. Wigger, S. Shamai, and H. V. Poor, "Joint coding of eMBB and URLLC in vehicle-to-everything (V2X) communications," in *Proceedings of the IEEE Global Communications Conference*, Kuala Lumpur, Malaysia, pp. 1–6, 4–8 Dec. 2023..

[24] J. Wang, G. Xie, D. Xia, and B. Dai, "Feedback coding of URLLC in vehicle-to-everything (V2X) communications and its secrecy analysis," in *Proceedings of the IEEE Wireless Communications and Networking Conference*, Dubai, United Arab Emirates, pp. 01-06, 21–24 April, 2024.

[25] H. Nikbakht, M. Egan, and J.-M. Gorce, "Dirty paper coding for consecutive messages with heterogeneous decoding deadlines in the finite blocklength regime," in *Proceedings of the IEEE International Symposium on Information Theory*, pp. 2100–2105, Espoo, Finland, 26 June – 01 July, 2022.

[26] M. H. M. Costa, "Writing on dirty paper (Corresp.)," *IEEE Transactions on Information Theory*, vol. 29, no. 3, pp. 439–441, May 1983.

[27] H. Li, Z. Han, and H. V. Poor, "A broadcast channel framework for joint communications and sensing-part II: Superposition coding," in *Proceedings of the IEEE Global Communications Conference*, Kuala Lumpur, Malaysia, pp. 7381–7386, 4–8 Dec. 2023.

[28] H. V. Poor, *An introduction to signal detection and estimation*, Springer Science & Business Media, 2013.

[29] H. Nikbakht, M. Wigger, S. Shamai, and H. V. Poor, "Integrated sensing and communication in the finite blocklength regime," in *Proceedings of the IEEE International Symposium on Information Theory*, pp. 2790–2795, Athens, Greece, 07–12 July, 2024.

[30] S. Lv et al., "Short-packet transmission in NOMA-ISAC systems," *IEEE Transactions on Cognitive Communications and Networking*, 2025.

[31] X. Shen, N. Zhao, and Y. Shen, "On the performance tradeoff of an ISAC system with finite blocklength," in *Proceedings of the IEEE International Conference on Communications*, pp. 4628–4633, Rome, Italy, 28 May-01 June, 2023.

[32] C. E. Shannon, "Probability of error for optimal codes in a Gaussian channel," *The Bell System Technical Journal*, vol. 38, no. 3, pp. 611–656, 1959.

[33] E. MolavianJazi and J. N. Laneman, "A second-order achievable rate region for Gaussian multi-access channels via a central limit theorem for functions," *IEEE Transactions on Information Theory*, vol. 61, no. 12, pp. 6719–6733, Dec. 2015.

[34] Y. Polyanskiy, "Channel coding: non-asymptotic fundamental limits", Ph.D. dissertation, Princeton University, Sep. 2010.

[35] Y. Polyanskiy, H. V. Poor and S. Verdú, "Channel coding rate in the finite blocklength regime," *IEEE Transactions on Information Theory*, vol. 56, no. 5, pp. 2307–2359, May, 2010.